Journal of Paleontology, 93(5), 2019, p. 971–1000

0022-3360/19/1937-2337
doi: 10.1017/jpa.2019.18

JOURNAL OF PALEONTOLOGY
A PUBLICATION OF THE Paleontological SOCIETY

Marine Early Triassic Actinopterygii from the Candelaria Hills (Esmeralda County, Nevada, USA)

Carlo Romano,[1] Adriana López-Arbarello,[2] David Ware,[1,3] James F. Jenks,[4] and Winand Brinkmann[1]

[1]Paläontologisches Institut und Museum, Universität Zürich, Karl Schmid-Strasse 4, 8006 Zürich, Switzerland, ⟨carlo.romano@pim.uzh.ch⟩; ⟨wbrink@pim.uzh.ch⟩
[2]Department für Geo- und Umweltwissenschaften (Paläontologie & Geobiologie), GeoBio-Center, Ludwig Maximilians Universität, Richard-Wagner-Straße 10, 80333 München, Germany, ⟨a.lopez-arbarello@lrz.uni-muenchen.de⟩
[3]Museum für Naturkunde, Leibniz-Institut für Evolutions- und Biodiversitätsforschung, Invalidenstraße 43, 10115 Berlin, Germany, ⟨david.ware@mfn-berlin.de⟩
[4]1134 Johnson Ridge Lane, West Jordan, Utah 84084, USA, ⟨jenksjimruby@comcast.net⟩

Abstract.—A new locality for low-latitudinal, Early Triassic fishes was discovered in the Candelaria Hills, southwestern Nevada (USA). The fossils are derived from the lower Candelaria Formation, which was deposited during the middle–late Dienerian (late Induan), ca. 500 ka after the Permian-Triassic boundary mass extinction event. The articulated and disarticulated Osteichthyes (bony fishes), encompassing both Actinistia (coelacanths) and Actinopterygii (ray-fins), are preserved in large, silicified concretions that also contain rare coprolites. We describe the first actinopterygians from the Candelaria Hills. The specimens are referred to *Pteronisculus nevadanus* new species (Turseoidae?), *Ardoreosomus occidentalis* new genus new species (Ptycholepidae), the stem neopterygian *Candelarialepis argentus* new genus new species (Parasemionotidae), and Actinopterygii indet. representing additional taxa. *Ardoreosomus* n. gen. resembles other ptycholepids, but differs in its more angulate hyomandibula and lack of an elongate opercular process. *Candelarialepis* n. gen. is one of the largest parasemionotids, distinguished by its bipartite preopercle and scale ornamentation. Presented new species belong to genera (*Pteronisculus*) or families (Ptycholepidae, Parasemionotidae) that radiated globally after the mass extinction, thus underlining the striking similarities between Early Triassic (pre-Spathian) osteichthyan assemblages. The current data suggest that the diversity of low-latitudinal, Early Triassic bony fishes may have been greater than indicated thus far by the fossil record, probably due to sampling or taphonomic failure. All 24 fossils from the Candelaria Hills represent mid-sized or large osteichthyans, confirming the obvious absence of very small species (≤ 10 cm adult body length) in the beginning of the Mesozoic Era—even in low latitudes.

UUID: http://zoobank.org/6a66ac96-d6b7-4617-94db-5a93cdb14215

Introduction

Why was the diversity of bony fishes highest in mid-latitudes during the Early Triassic? Why were bony fishes overall larger in the Early Triassic than in the Middle Triassic? Regardless of recent research progress, there are still open questions concerning the radiation of fishes after the Permian-Triassic boundary mass extinction event (PTBME; 251.959 ± 0.018 Ma; Baresel et al., 2017). This catastrophic event was accompanied by global climatic and environmental shifts and is considered an analog for the Anthropocene climate change and biodiversity loss (Payne and Clapham, 2012). The same concept is applicable to the extensively studied, Early Triassic post-extinction interval, which was marked by CO_2-driven climatic turmoil, associated biotic crises, and subsequent blooms (e.g., Brayard et al., 2006, 2017; Romano et al., 2013; Hofmann et al., 2014; Scheyer et al., 2014). Despite the similarities, some attributes of the current 'sixth mass extinction' are unprecedented (Ceballos and Ehrlich, 2018; Payne et al., 2016).

Although the PTBME had only minor impact on non-tetrapod bony fishes (piscine Osteichthyes), the latter greatly diversified during the subsequent biotic recovery (e.g., Romano et al., 2016a; Smithwick and Stubbs, 2018). However, their spatiotemporal pattern of dispersal is obscured because some paleogeographic domains suffer from an incomplete record (López-Arbarello, 2004; Brinkmann et al., 2010; Romano et al., 2016b, 2017), and because of uncertainties regarding the phylogenetic relationships of several taxa. One geographic domain affected by scarce data is the low-paleolatitudinal belt (30°N to 30°S of the paleoequator; Romano et al., 2016a). Whether the aforesaid, depauperate diversity in low-latitudes compared to mid-latitudes (30–60°N and 30–60°S) reflects a biological signal, for instance extreme temperatures, or whether it derives from sampling or taphonomic bias, requires scrutiny (cf., Romano et al., 2017). Likewise, the body-size distribution of osteichthyans during the Lopingian (late Permian) and Early Triassic, which was atypically skewed towards large-sized species (Romano et al., 2016a; Puttick et al., 2017), needs further investigation. The increased representation of large-sized taxa in the Early Triassic could be related to very limited data from low-latitudinal collecting localities, because tropical fishes typically tend to be smaller than those in higher latitudes (Fisher

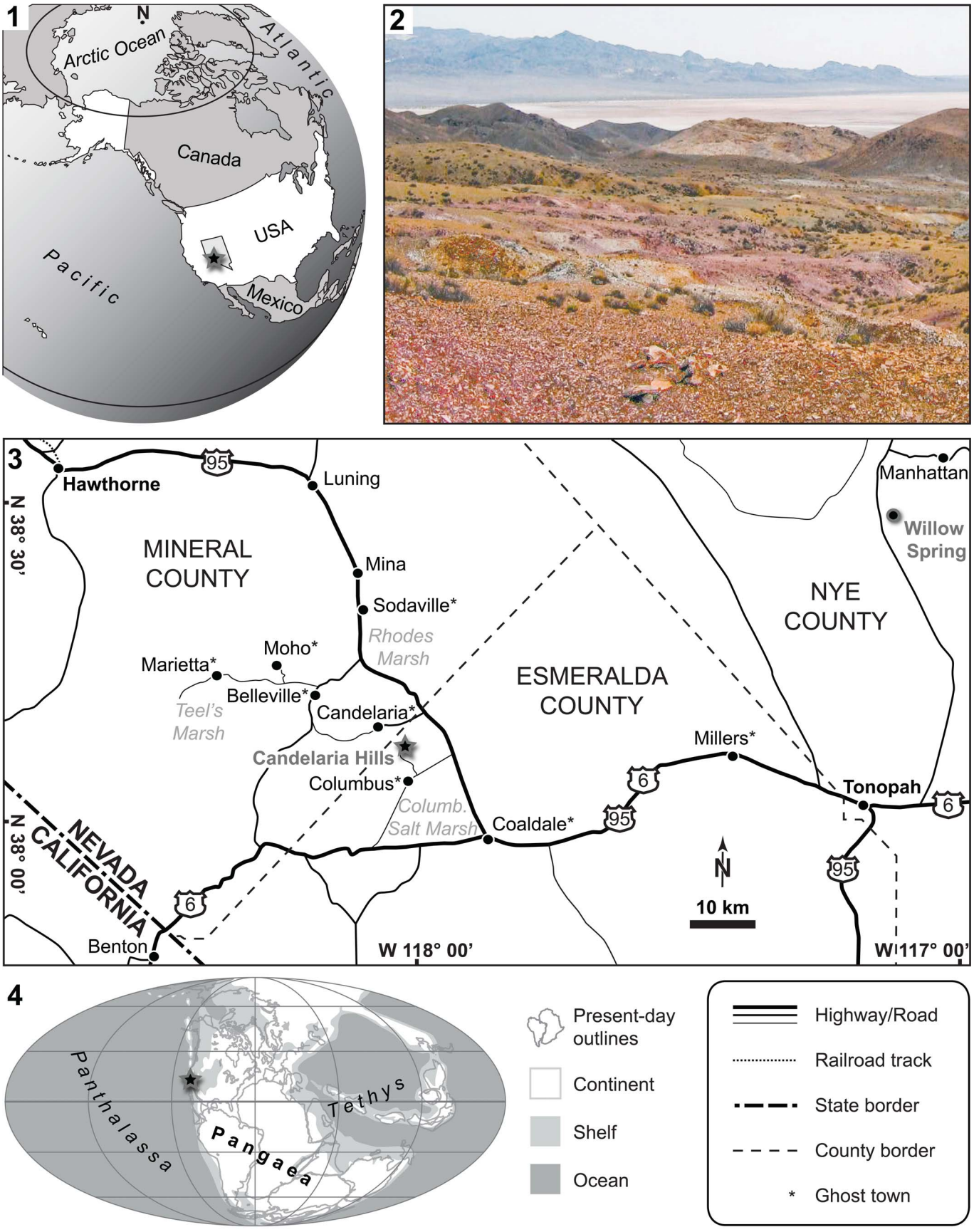

https://doi.org/10.1017/jpa.2019.18 Published online by Cambridge University Press

Figure 1. The study site. (**1**) Map of the United States of America (state of Nevada highlighted in bright gray); (**2**) study site in the Candelaria Hills (color photo online): view towards the southeast, the Columbus Salt Marsh is seen in the background, cluster of fish-bearing nodules in the foreground are each ~20–30 cm in diameter; (**3**) map of southwestern Nevada (figure legend bottom right); (**4**) Early Triassic paleogeographic map (modified from PALEOMAP project, www.scotese.com). The black-gray stars in **1.1, 1.3**, and **1.4** indicate the location of the study site. The black-gray circle in **1.3** indicates Willow Spring (Nye County, Nevada), from where fish teeth have been reported previously. See text for details.

et al., 2010). The Middle Triassic record, in contrast, indicates a body size distribution skewed towards small-bodied forms (Deecke, 1927; Bürgin, 1999; Tintori et al., 2014; Romano et al., 2016a). This significant shift may be due to a surge in taxa with body lengths of only a few centimeters, many of which pertain to Neopterygii, the most diverse clade in modern aquatic ecosystems (Sallan, 2014; Clarke and Friedman, 2018; Smithwick and Stubbs, 2018). Yet, sampling bias again cannot be dismissed because the Middle Triassic record is heavily based on low-latitudinal occurrences, including exceptional Lagerstätten (Tintori et al., 2014).

A new, productive locality preserving low-latitudinal, Early Triassic bony fishes was recently discovered in the old Candelaria silver mining district in Nevada (USA). The objective of the present paper is to describe the first actinopterygians from this site and to discuss the new findings in the context of latitudinal diversity distribution and body size changes in the aftermath of Earth's most severe mass extinction event of the past.

Geological setting

Locality.—The fishes described below were found in the Candelaria Hills, a low mountain range situated south of the long-abandoned mining boom town of Candelaria (Mineral County, Nevada, USA; Fig. 1). To the east, the Candelaria Hills extend into Esmeralda County of Nevada. The present material was collected from a locality in the eastern portion of the Candelaria Hills, just north of the ghost town of Columbus (Esmeralda County). The site is located west of US Route 95, about halfway between Tonopah (Nye County, Nevada) and Hawthorne (Mineral County). The GPS coordinates of the collecting locality are N38°07′53.9″, W118°01′32.6″ (township/range coordinates: NE1/4, Sec 12, T3N, R35E).

Geology and age.—The fishes are derived from the lower part of the ~1000 m thick (Muller and Ferguson, 1939) Candelaria Formation, of Dienerian age (Ware et al., 2011). We use Tozer's (1965) Early Triassic stage subdivision, which is supported by detailed biozonations (e.g., Ware et al., 2015): Griesbachian (early Induan), Dienerian (late Induan), Smithian (early Olenekian), and Spathian (late Olenekian). The Candelaria Formation crops out in several places in the Candelaria Hills, and fish remains have been noted in different sites (personal observation, DW, JFJ; H. Bucher, personal communication, 2011). The Candelaria Formation is also exposed in Willow Spring (Toquima Range, Nye County; Fig. 1.3), from where Poole and Wardlaw (1978) listed the presence of fish teeth, but without more details.

Muller and Ferguson (1939) were the first to mention the occurrence of invertebrate fossils in the lower Candelaria Formation. These authors noted the presence of two different molluscan faunas: a lower assemblage comprising several species of the bivalve *Claraia*, Bittner, 1901, and an upper fauna with ammonoids. Ware et al. (2011) described for the first time ammonoids from the lower Candelaria Formation, and they identified three different horizons. The first (lowest) fauna, within the *Claraia* beds, includes *Ambites subradiatus* Ware and Bucher in Ware et al., 2018a, characteristic of the middle Dienerian *A. discus* Regional Zone of Ware et al. (2018a, b) and unitary-association-zone (UA-zone) DI-6 of Ware et al. (2015). The second fauna, where most of the ammonoids described by Ware et al. (2011) come from, contains *A. lilangensis* (von Krafft in von Krafft and Diener, 1909) and correlates with the late middle Dienerian *A. lilangensis* Regional Zone of Ware et al. (2018a, b) and UA-zone DI-8 of Ware et al. (2015). The third fauna includes *Vavilovites meridialis* Ware and Bucher in Ware et al., 2018b, the typical species of the *V.* cf. *sverdrupi* Regional Zone of Ware et al. (2018a), the *V. meridialis* Regional Zone of Ware et al. (2018b), and UA-zone DI-9 of Ware et al. (2015), of early late Dienerian age.

The specimens studied herein come from a different outcrop in the Candelaria Hills than the mollusks described by Ware et al. (2011). At the study site, the outcrop is not well exposed and covered by scree (Fig. 1.2), except in a few shallow, seasonal stream channels, thus preventing the measurement of a stratigraphic section. Based on observations of in situ collected material, the bedding plane is nearly parallel to the local topography, so that all specimens are assumed to originate from a single horizon. The difference in composition (e.g., silicate concretions for fishes versus carbonate nodules for the ammonoids of Ware et al., 2011) is most likely secondary and linked to abundant hydrothermal circulation and dikes, which are interspersed throughout the sedimentary deposits (there are concessions exploiting turquoise and there used to be silver mines nearby; e.g., Knopf, 1922; Page, 1959).

Although conodonts were reported from the Candelaria Formation (Collinson and Hasenmueller, 1978; Poole and Wardlaw, 1978), they may have been dissolved diagenetically at the study site (like the fish bones) because none could be detected in the matrix surrounding the fishes. A few external molds of ammonoids occur with the fishes (e.g., PIMUZ A/I 4730), but they are either indeterminable juveniles or poorly preserved. At the study sites of Ware et al. (2011), isolated bones (PIMUZ 35926) were found together with the late middle Dienerian (sensu Ware et al., 2015) *A. lilangensis* fauna, and it is probable that the fishes described herein are from the same horizon. The fishes clearly come from the lower Candelaria Formation, which is middle to late Dienerian in age (late Induan, early Early Triassic).

Paleoenvironment.—The Early Triassic paleogeography was characterized by the Pangean supercontinent, which was surrounded by the Panthalassa and Tethys oceans. The study

https://doi.org/10.1017/jpa.2019.18 Published online by Cambridge University Press

locality was situated in low latitudes in the eastern Panthalassa (Fig. 1.4), probably plate-bound (Ware et al., 2011), but the region to the west of the site was marked by terranes and volcanism (Poole and Wardlaw, 1978; Wyld, 2000). The relationships between the study site and the western USA epicontinental sea (= Sonoma Foreland Basin), from which the slightly younger fish occurrences in northeast Nevada and Idaho were described (e.g., Romano et al., 2012, 2017, in press), are difficult to reconstruct due to the complex tectonic context (Page, 1959; Wyld, 2000). The lower Candelaria Formation was deposited in a moderately deep outer shelf setting, in a basinal trough characterized by high sedimentation rates (Poole and Wardlaw, 1978). The dark, laminated, organic-rich shale is indicative of oxygen-depleted bottom waters; in fact, evidence for anoxia on outer shelves during the middle and late Dienerian was documented worldwide (see Ware et al., 2015 and references therein). The anoxic conditions favored good preservation of the fishes.

Materials and methods

Materials and preservation.—The occurrence of articulated fishes in the Candelaria Hills was discovered in 2008 by JFJ and DW (Brinkmann et al., 2010; Ware et al., 2011), and a survey of the site was undertaken in 2009. We collected a total of 24 osteichthyan specimens (mostly fragmentary crania), which are curated in part by the New Mexico Museum of Natural History and Science, Albuquerque, New Mexico, USA (specimens NMMNH P-57422 and P-57423), and in part by the Paleontological Institute and Museum, University of Zurich, Switzerland (PIMUZ A/I 4402, A/I 4718 to A/I 4733, other specimens). The material includes actinistians (coelacanths) and actinopterygians (ray-fins), as well as coprolites (~2 cm in diameter; PIMUZ A/I 4729). Seven actinopterygian specimens are described herein, while the actinistians, which represent the bulk of the collected material (11 out of 19 workable osteichthyan remains), will be described separately.

The fishes from the Candelaria Formation are preserved as external molds in silicified, early diagenetic concretions. The often large nodules occur mostly as float, but can also be found in situ within the bituminous shale, colored purplish on the surface due to weathering (Fig. 1.2). The fish skeletons display varying degrees of completeness and disarticulation, ranging from largely articulated to entirely disarticulated. The disarticulated specimens suggest floatation in warm surface water after the animals died, whereas articulated individuals indicate death in deeper, cooler water (Anderson and Woods, 2013).

Terminology.—For better comparability with previous descriptions, we herein apply the classic bone terminology of fossil actinopterygians (e.g., Nielsen, 1942; Lehman, 1952; Bürgin, 1992; Grande and Bemis, 1998), but homologies with similarly named elements of other vertebrates are not necessarily implied (cf., Schultze, 2008; Mickle, 2013, 2015). Regarding the lateral scales, we refer to length as their longitudinal (anteroposterior) and to depth/height as their dorsoventral extension. For scales of the dorsal and ventral midlines, we refer to the lateral dimension as width. The terms 'palaeoniscoid' and 'subholostean' refer to general body bauplans and are herein applied without phylogenetic meaning. For the sake of convenience, whenever we refer to Osteichthyes (bony fishes) in the text, only the non-tetrapod (or piscine) members of this clade are meant.

Repositories and institutional abbreviations.—BSPG, Bayerische Staatssammlung für Paläontologie und Geologie, Munich, Germany; MNHN.F, Muséum National d'Histoire Naturelle, Paris, France; NMMNH, New Mexico Museum of Natural History and Science, Albuquerque, New Mexico, USA; NMNH, Smithsonian's National Museum of Natural History, Washington D. C., USA; PIMUZ, Paleontological Institute and Museum, University of Zurich, Zurich, Switzerland; PMU, Museum of Evolution, Uppsala University, Uppsala, Sweden.

Systematic paleontology

Class Osteichthyes Huxley, 1880
Subclass Actinopterygii Cope, 1887, emend. Rosen et al., 1981
Family Turseoidae? Bock, 1959
Genus *Pteronisculus* White, 1933

Type species.—*Pteronisculus cicatrosus* White, 1933; from the Early Triassic of northwest Madagascar.

Occurrence.—See Table 1.

Remarks.—*Pteronisculus* White, 1933 (sensu Nielsen, 1942) is a synonym of *Glaucolepis* Stensiö, 1921, which is preoccupied (White and Moy-Thomas, 1940). The type species of '*Glaucolepis*,' '*G.*' *gyrolepidoides* Stensiö, 1921 from the Early Triassic of Spitsbergen (Svalbard), is poorly known (Véran, 1988). *Pteronisculus* has been referred to Palaeoniscidae Vogt, 1851 (for family diagnosis see Aldinger, 1937) by several authors (e.g., Stensiö, 1932; Nielsen, 1942; Lehman, 1952; Schaeffer, 1967; Gardiner and Jubb, 1975). It was recently excluded from this family and reclassified as a stem actinopteran incertae sedis (Xu et al., 2014). These authors consider *Palaeoniscum* Blainville, 1818 more derived than *Pteronisculus*. Schaeffer (1952) pointed out resemblances between *Pteronisculus* and *Turseodus* Leidy, 1857 (= *Gwyneddichtis* Bock, 1959; *Eurecana* Bock, 1959; see Schaeffer, 1967 for synonymy) from Late Triassic freshwater deposits of the United States. Apart from general similarities (skull bone pattern, fins), he mentions an anterior infraorbital bone bearing teeth in *Turseodus* (Schaeffer, 1952). Because the contribution of the lachrymal to the oral margin is considered an autapomorphy of *Pteronisculus* (Xu et al., 2014), the two genera are here tentatively included in the same family, Turseoidae Bock, 1959. *Pteronisculus* differs from *Turseodus* in its shorter anal fin base and lack of ossified vertebral centra (Schaeffer, 1952, 1967; Bock, 1959). The Permian *Turfania* Liu and Ma, 1973 might be referable to the

https://doi.org/10.1017/jpa.2019.18 Published online by Cambridge University Press

Table 1. Occurrences of species of *Pteronisculus* White, 1933, according to the published literature. Species are listed in chronology of their first description. See text for details.

Species	Occurrence	Age	References
P.? *laetus*	Alberta (Canada)	Early Triassic	Lambe (1916), Stensiö (1921), Aldinger (1937), Gardiner (1966), Schaeffer and Mangus (1976), Neuman (2015)
P. gyrolepidoides	Spitsbergen (Svalbard)	Early Triassic	Stensiö (1921), Véran (1988)
P. cicatrosus	Northwest Madagascar	Early Triassic	White (1933), Lehman (1952), Uyeno (1978)
P. arcticus	Greenland	Early Triassic	Stensiö (1932), Nielsen (1936, 1942)
P. stensioi	Greenland	Early Triassic	Nielsen (1942)
P. gunnari	Greenland	Early Triassic	Nielsen (1942)
P. magnus	Greenland	Early Triassic	Nielsen (1942)
P. aldingeri	Greenland	Early Triassic	Nielsen (1942)
P. macropterus	Northwest Madagascar	Early Triassic	White (1933), Lehman (1952)
P. arambourgi	Northwest Madagascar	Early Triassic	Lehman (1952)
P. broughi	Northwest Madagascar	Early Triassic	Lehman (1952)
P. cf. *macropterus*	Northwest Madagascar	Early Triassic	Beltan (1968)
P. ? *meiringi*	South Africa	Lopingian	Gardiner and Jubb (1975), Bender (2004)
Pteronisculus? sp.	British Columbia (Canada)	Early Triassic	Schaeffer and Mangus (1976), Neuman (2015)
P. nielseni	Yunnan (China)	Middle Triassic	Xu et al. (2014)
P. nevadanus n. sp.	Nevada (USA)	Early Triassic	this study

same family on the basis of the similar cranial bone pattern, including the position of the lachrymal (antorbital).

Pteronisculus nevadanus new species
Figures 2–4

Holotype.—PIMUZ A/I 4402, preserved as part (A/I 4402a; Figs. 2, 4) and counterpart (A/I 4402b; Fig. 3). Silicone casts of parts a and b were produced for this study. Specimen A/I 4402a is associated with an indeterminable ammonoid fragment.

Differential diagnosis.—Small to mid-sized species of *Pteronisculus*; postorbital portion of maxilla low and elongate (relatively shorter and higher in *P. arcticus* [Stensiö, 1932], *P. aldingeri* [Nielsen, 1942], *P. nielseni* Xu, Shen, and Zhao, 2014); dorsal margin of postorbital blade of maxilla concave (straight in *P. cicatrosus, P. magnus* [Nielsen, 1942], *P. gunnari* [Nielsen, 1942], *P. nielseni*; convex in *P. stensioi* [Nielsen, 1942]); Meckel's cartilage only ossified in its most posterior portion (ossified throughout its length in the Greenlandic and Madagascan species); two coronoids present, both about as large as the prearticular (coronoids smaller than prearticular in *P. magnus*, *P. cicatrosus*, *P. macropterus* White, 1933); teeth absent in the posterior part of the internal lamina of the maxilla (teeth present in *P. macropterus*, *P. arambourgi* Lehman, 1952, *P. magnus*); suborbitals consisting of one large dorsal element and several smaller elements ventral to it (different numbers and configurations in other species); ornamentation of dermal bones consisting mostly of tubercles (like in *P. magnus*, *P. aldingeri*, *P. cicatrosus*, *P. arambourgi*, *P. broughi* Lehman, 1952; mostly striae in *P. arcticus*, *P. stensioi*, *P. gunnari*, *P. macropterus*, *P. nielseni*); ornamentation of opercle relatively weak (strong in *P. magnus*); ornamentation of scales composed of oblique striae (predominantly tubercles in *P. broughi*); number of pectoral fin rays (~27) similar to *P. cicatrosus* (~26) (more numerous in *P. magnus* [45–50], *P. arcticus*, *P. stensioi*, and *P. gunnari* [35–40], *P. macropterus* [35], or *P. arambourgi* [31], less numerous in *P.*? *meiringi* Gardiner and Jubb, 1975 [20–22], distinctly less numerous in *P. nielseni* [15]); number of pelvic fin rays (~23) comparable to *P. stensioi* (19–24) (less numerous in *P. arcticus* [17], *P. gunnari* [18–20], *P. aldingeri* [18], and *P. nielseni* [14]).

Occurrence.—From the lower Candelaria Formation (middle-upper Dienerian, Lower Triassic) of the eastern Candelaria Hills (Esmeralda County, Nevada, USA).

Description.—PIMUZ A/I 4402 is partly disarticulated but relatively complete.

Jaws.—Both palatoquadrates are visible (Figs. 2, 3), but incompletely preserved. The right palatoquadrate is preserved in situ, while the left one is still attached to the dislocated dermal upper jaw bones. On the medial side of the left maxilla (A/I 4402b; Fig. 3), a single, slender dermopalatine and a fragmentary entopterygoid are seen. The elongate entopterygoid exhibits an oblique anterodorsal margin, dorsal to which the palatoquadrate is exposed. The lingual surfaces of the entopterygoid and dermopalatine show numerous minute teeth. The premaxilla is absent, but both maxillae are visible. Whereas the right maxilla is preserved in situ, the left one is found isolated anteroventral to the rest of the fossil. The latter is still attached to the palatoquadrate, entopterygoid, dermopalatine, and preopercle. The maxilla is cleaver-shaped, consisting of an expanded postorbital plate, and a short, slender anterior process, which rostrally bends medially. The elongate, relatively low postorbital blade is bounded by four margins. Its dorsal and anterodorsal borders are both concave. They meet in an obtuse angle. The posterior margin of the postorbital plate is straight and runs obliquely from anterodorsal to posteroventral in its upper part. In its lower portion, the posterior margin is more vertically oriented and marked by a posterior notch. The ventral margin of the maxilla is S-shaped, being concave in its posterior segment and convex in its anterior portion. The ornamentation of the postorbital plate of the maxilla consists of coarse tubercles, which gain in size in the posteroventral part of the bone (Fig. 4.1). A narrow, unornamented area along the anterior margin of the postorbital plate was in vivo laterally covered by the suborbitals. The anterior process of the maxilla does not show dermal ornament. The bases of small teeth are visible along the ventral margin of the postorbital blade of the left maxilla, and a strong internal (horizontal) lamina is preserved on the

https://doi.org/10.1017/jpa.2019.18 Published online by Cambridge University Press

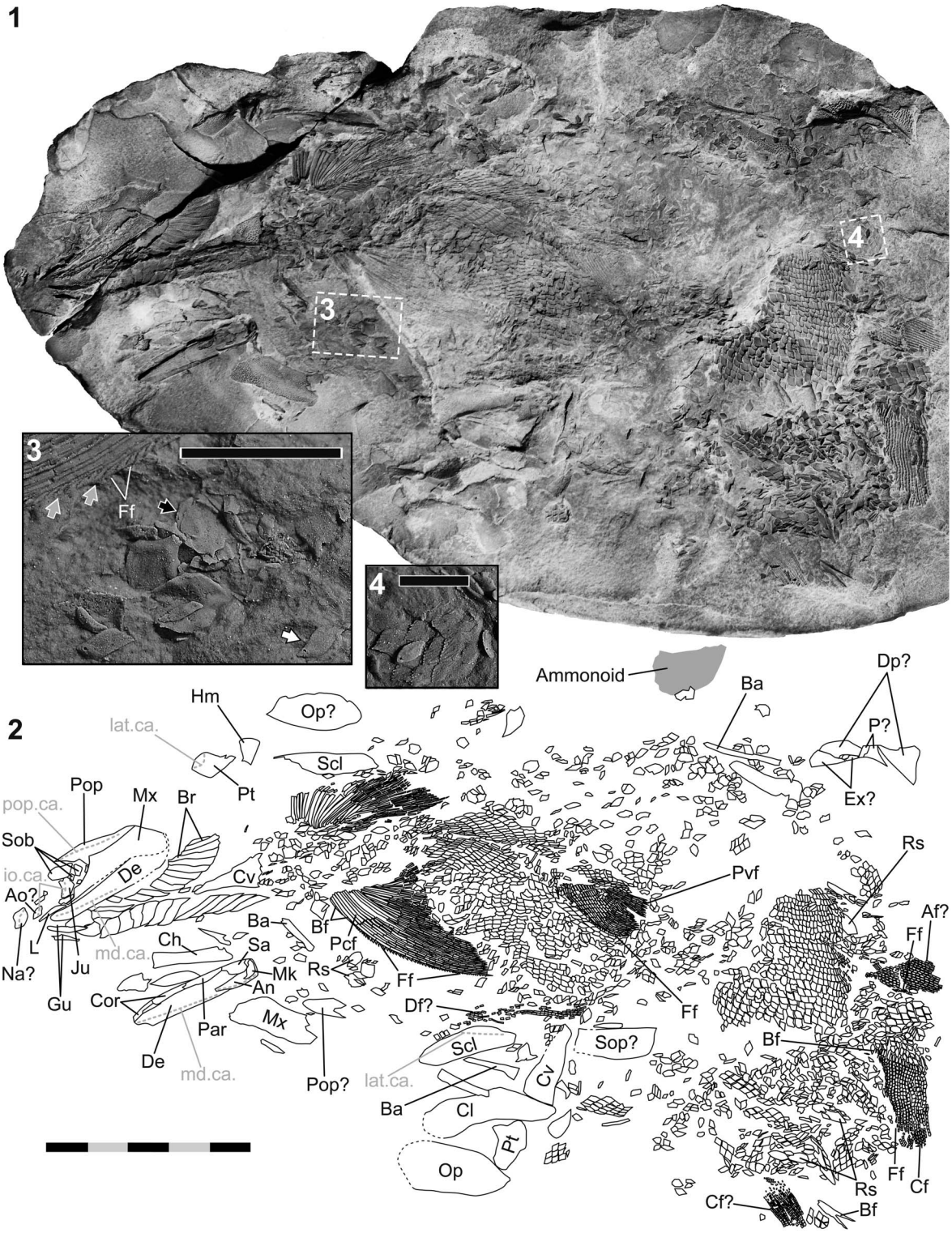

Figure 2. *Pteronisculus nevadanus* n. sp. from the middle-late Dienerian of the Candelaria Hills (Esmeralda County, Nevada, USA). (**1**) Part a of PIMUZ A/I 4402 (holotype; enhanced with ammonium chloride); (**2**) interpretive line drawing of **2.1** (segmentation and branching of fin rays simplified), with interpretations of skeletal elements; (**3**) close-up view (silicone cast of PIMUZ A/I 4402a; position indicated in **2.1**) of a portion of the left pectoral fin, with intercalated tip segments of lepidotrichia (gray arrows) mimicking fringing fulcra (Pattern B of Arratia, 2009), and a few isolated, ellipsoid ridge scales (black arrow), and rhombic scales with dorsal spines (white arrow); (**4**) close-up view (silicone cast of PIMUZ A/I 4402a; position indicated in **2.1**) of a patch of rhombic scales showing ornamentation of the free field. Anterior is left in **2.1** and **2.2**, and right in **2.3** and **2.4**. Scale bar is 50 mm (total) in **2.1** and **2.2**, 10 mm in **2.3**, and 5 mm in **2.4**. Abbreviations: **Af**, anal fin (lepidotrichia); **An**, angular; **Ao**, antorbital; **Ba**, branchial arch element; **Bf**, basal fulcrum; **Br**, branchiostegal ray; **Cf**, caudal fin (lepidotrichia); **Ch**, ceratohyal; **Cl**, cleithrum; **Cor**, coronoid; **Cv**, clavicle; **De**, dentary; **Df**, dorsal fin (lepidotrichia); **Dp**, dermopterotic; **Ex**, extrascapular; **Ff**, fringing fulcrum; **Gu**, gular plate (median/lateral); **Hm**, hyomandibula; **io.ca.**, infraorbital sensory canal; **Ju**, jugal; **L**, lachrymal; **lat.ca.**, lateral line sensory canal; **md.ca.**, mandibular sensory canal; **Mk**, Meckel's cartilage (ossified as the articular); **Mx**, maxilla; **Na**, nasal; **Op**, opercle; **P**, parietal; **Par**, prearticular; **Pcf**, pectoral fin (lepidotrichia); **Pop**, preopercle; **pop.ca.**, preopercular sensory canal; **Pt**, posttemporal; **Pvf**, pelvic fin (lepidotrichia); **Rs**, ridge scale; **Sa**, supraangular; **Scl**, supracleithrum; **Sob**, suborbital bone; **Sop**, subopercle.

https://doi.org/10.1017/jpa.2019.18 Published online by Cambridge University Press

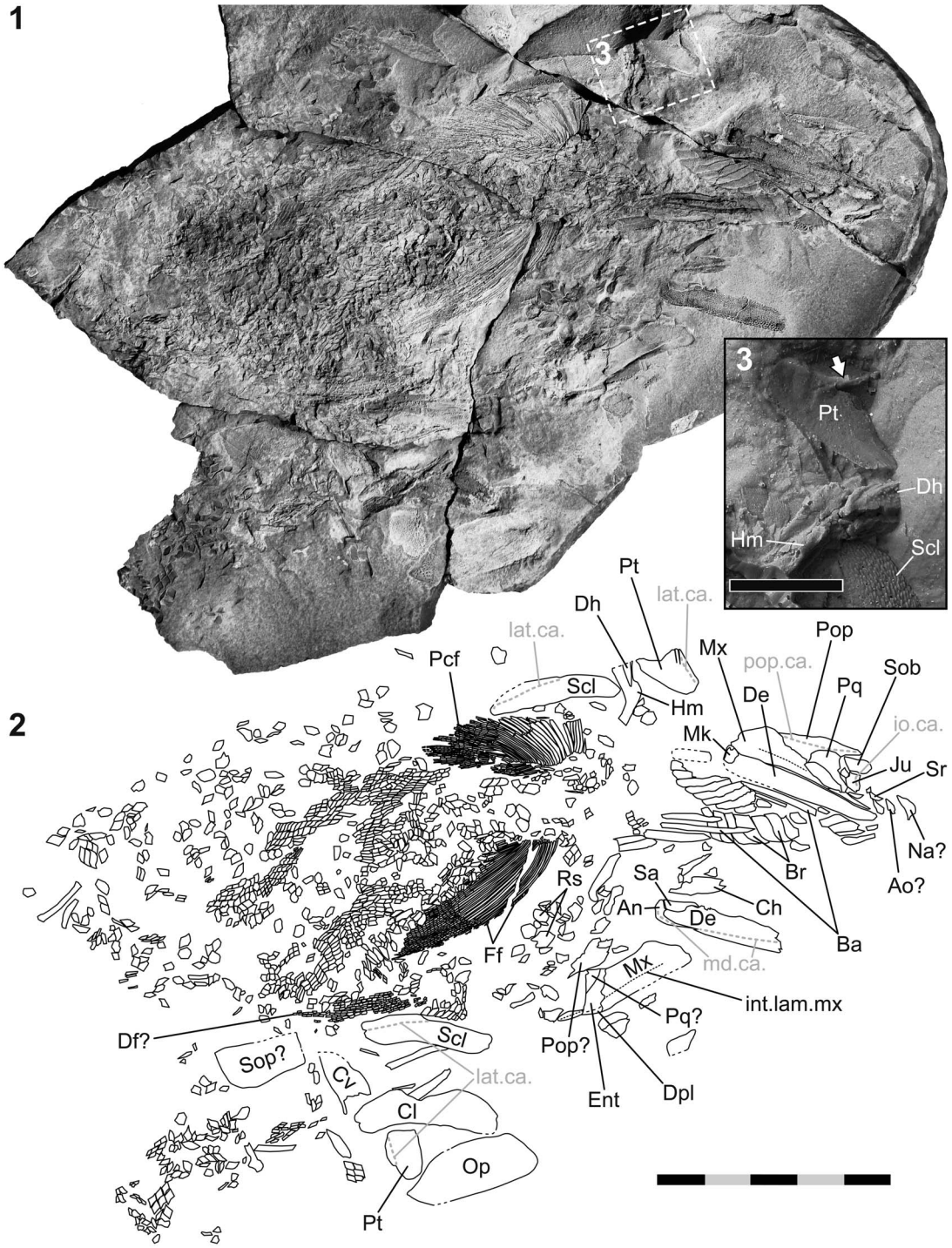

Figure 3. *Pteronisculus nevadanus* n. sp. from the middle-late Dienerian of the Candelaria Hills (Esmeralda County, Nevada, USA). (**1**) Part b of PIMUZ A/I 4402 (holotype; enhanced with ammonium chloride); (**2**) interpretive line drawing of **3.1** (segmentation and branching of fin rays simplified), with interpretations of the skeletal elements; (**3**) close-up of the right hyomandibula, dermohyal, and posttemporal (silicone cast of PIMUZ A/I 4402b). Anterior is right in **3.1** and **3.2**, and top left in **3.3**. The white arrow in **3.3** points to the ventral process of the posttemporal. Scale bar measures 50 mm (total) in **3.1** and **3.2**, and 10 mm in **3.3**. Abbreviations: **An**, angular; **Ao**, antorbital; **Ba**, branchial arch element; **Br**, branchiostegal ray; **Ch**, ceratohyal; **Cl**, cleithrum; **Cv**, clavicle; **De**, dentary; **Df**, dorsal fin (lepidotrichia); **Dh**, dermohyal; **Dpl**, dermopalatine; **Ent**, entopterygoid; **Ff**, fringing fulcrum; **Hm**, hyomandibula; **int.lam.mx.**, internal lamina of the maxilla; **io.ca.**, infraorbital sensory canal; **Ju**, jugal; **lat.ca.**, lateral line sensory canal; **md.ca.**, mandibular sensory canal; **Mk**, Meckel's cartilage (ossified as the articular); **Mx**, maxilla; **Na**, nasal; **Op**, opercle; **Pcf**, pectoral fin (lepidotrichia); **Pop**, preopercle; **pop.ca.**, preopercular sensory canal; **Pq**, palatoquadrate; **Pt**, posttemporal; **Rs**, ridge scale; **Sa**, supraangular; **Scl**, supracleithrum; **Sob**, suborbital bone; **Sop**, subopercle; **Sr**, sclerotic ring element.

medial side of both maxillae (A/I 4402b; Fig. 3). Within the rostral process, the internal lamina closely follows the ventral margin of the maxilla, whereas in the postorbital plate, the lamina is distinctly offset to the ventral border. The internal lamina does not carry teeth in its posterior section, but small teeth are developed in its suborbital portion.

https://doi.org/10.1017/jpa.2019.18 Published online by Cambridge University Press

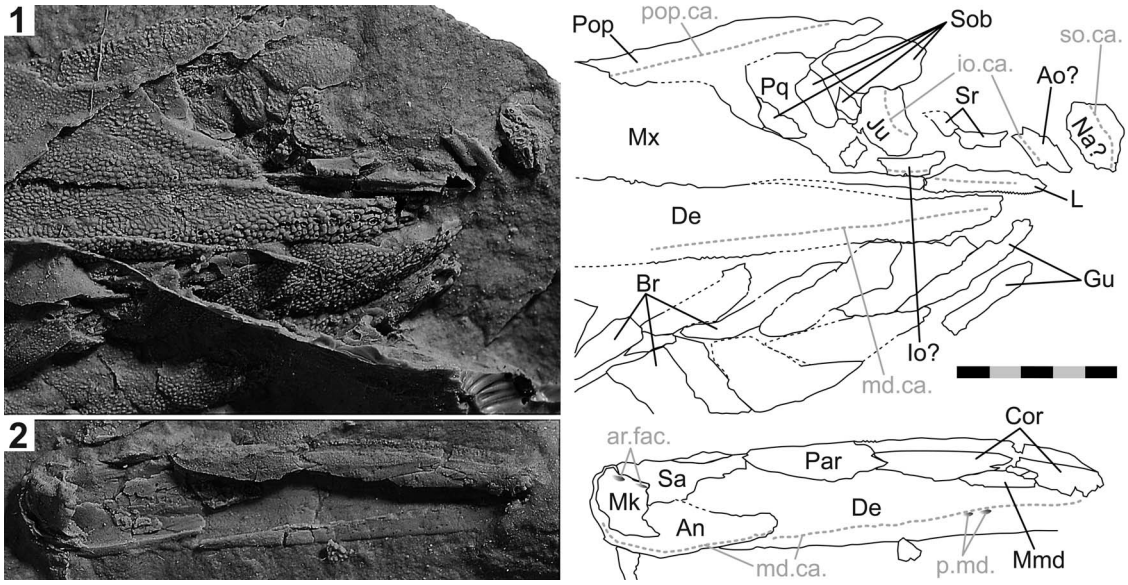

Figure 4. *Pteronisculus nevadanus* n. sp. (silicone cast of part a of PIMUZ A/I 4402, holotype) from the middle-late Dienerian of the Candelaria Hills (Esmeralda County, Nevada, USA). (**1**) Bones of the right cheek region and neighboring areas in lateral view (left), with a drawing and interpretation thereof (right); (**2**) left mandible in medial view (left), with interpretive drawing of the bones (right). Anterior is right. Scale bar measures 10 mm (total). Abbreviations: **An**, angular; **Ao**, antorbital; **ar.fac.**, facet on the articular for jaw articulation; **Br**, branchiostegal ray; **Cor**, coronoid; **De**, dentary; **Gu**, gular plate (median/lateral); **Io**, infraorbital bone; **io.ca.**, infraorbital sensory canal; **Ju**, jugal; **L**, lachrymal; **md.ca.**, mandibular sensory canal; **Mk**, Meckel's cartilage (ossified as the articular); **Mmd**, 'medial bone in the anterior part of the mandible' (Nielsen, 1942); **Mx**, maxilla; **Na**, nasal; **Par**, prearticular; **p.md.**, 'depression on the medial side of the dentary' (Nielsen, 1942); **Pop**, preopercle; **pop.ca.**, preopercular sensory canal; **Pq**, palatoquadrate; **Sa**, supraangular; **so.ca.**, supraorbital sensory canal; **Sob**, suborbital bone; **Sr**, sclerotic ring element.

Both rami of the lower jaw are preserved. The right one is still in situ and the left one is found isolated. The mandible is curved medially throughout its length, but most distinctly in its rostral portion. The lateral side of the lower jaw, which is best seen on the left mandible on part b (Fig. 3), consists of three bones: dentary, angular, and surangular. The dentary is the largest of these elements. Laterally, it extends from the rostral tip of the lower jaw to almost the posterior margin. Several fairly small teeth are preserved along the dorsal margin of the dentary, arranged in more or less two rows (Fig. 4.2). The angular forms the posterior and posteroventral edge of the mandible. It has a triangular outline in medial view (Fig. 4.2); however, it is mostly covered by the dentary laterally, with only its marginal posterior and posteroventral portions exposed (Fig. 3). The surangular is located anterodorsal to the angular and posterodorsal to the dentary. It lacks a coronoid process. The mandibular sensory canal can be traced in the dentary and angular. This canal runs obliquely though the rostral portion of the dentary and successively approaches the ventral margin of this bone posteriorly. The canal pierces the angular through its anterior end and traverses this element close to its ventral and posterior margins. The ornamentation of the lower jaw consists of tubercles, which are particularly coarse in the rostral part, precisely in the region ventral to the mandibular sensory canal (Fig. 4.1). The surangular and adjacent, marginal areas of the dentary and angular lack ornamentation. The medial side of the lower jaw is visible on part a of the fossil (Figs. 2, 4.2). Lingually, the dentary does not reach as far posteriorly as on the lateral side. The part lying ventral to the mandibular sensory canal is thickened. Along the dorsal margin of the thickened portion, within the rostral part of the dentary, there are at least two oval depressions (Fig. 4.2) corresponding to the 'shallow depressions' of Nielsen (1942, p. 165).

There is a series of three bones medially adjoining the dorsal margin of the dentary (Fig. 4.2). The most posterior of these elements, which extends caudally until the surangular, represents the prearticular. The lingual surface of the prearticular is equipped with a row of small teeth in its anterior part, which are slightly smaller than the teeth on the dentary. The two bones rostral to the prearticular are the coronoids. The posterior coronoid is only slightly longer than the prearticular, while the anterior coronoid is shorter than the posterior one. The suture between the prearticular and the posterior coronoid is distinctly indented. The medial surfaces of both coronoids are smooth ventrally, whereas dorsally these bones are armed with minute teeth. Most dorsally, there is a single row of larger teeth, of comparable size to those on the prearticular. Ventral to the anterior and posterior coronoids is at least one additional element. It corresponds to the 'bone in the anterior part of the mandible' of Nielsen (1942, fig. 38). This element has a smooth lingual surface. In the living animal, the space delimited by the prearticular and coronoids dorsally, and the thickened lower portion of the dentary and angular ventrally, was occupied by Meckel's cartilage, the most posterior part of which is ossified as the articular. This bone is preserved in situ on both the left and the right mandible (Figs. 2, 3, 4). It is subtriangular in medial aspect and laterally connected to both the angular and surangular. Its dorsal surface is marked by two articulation facets (double jaw joint), best visible on the casts of A/I 4402a and b.

Preopercle and operculogular series.—Dorsal to the right maxilla, the upper branch of the corresponding preopercle is preserved (Figs. 2, 3, 4). The posteroventral shank of this bone is

https://doi.org/10.1017/jpa.2019.18 Published online by Cambridge University Press

not visible. The anterodorsal ramus of the preopercle is roughly triangular in outline, with a deeply concave anteroventral border, and a long, sigmoid dorsal margin, which is anteriorly convex and posteriorly concave. The ventral border of the anterodorsal shank is covered by the maxilla. The anterodorsal portion of the preopercle is elongate and pointed rostrally. The preopercular sensory canal pierces the anterodorsal shank slightly above the rostral tip of the bone and passes through the preopercle near its dorsal margin (Fig. 4.2). The ornamentation is composed of tubercles below the sensory canal, and subvertical striae and tubercles above it.

The operculogular series is mostly complete, but partly disarticulated (Figs. 2–4). The gulars and branchiostegals are found in situ. The gular plates are not well preserved, but seemingly three of them are developed—a narrow median gular and a pair of slightly broader lateral gulars. Posterior to the gular plates is a paired series of ~13 branchiostegal rays on either side. Each branchiostegal ray is elongate and relatively broad, similar to the gular plates. The breadth of the rays successively decreases towards the posterior elements. The gulars and branchiostegals overlap a marginal area of the caudally following element.

Two isolated, oval, plate-like bones are interpreted as the opercles. The left opercle is located ventral and the right opercle dorsal to the rest of the skeleton (Figs. 2, 3). Because the right opercle is poorly preserved, the description is based on the left one, which is exposed in lateral view. The opercle is the largest bone of the operculogular series. It is bounded by convex posterodorsal and anteroventral margins, a straight, short anterior border, and a distinctly convex posteroventral margin. Its anterodorsal end is pointed (the orientation is inferred from comparisons with other species, cf., Nielsen, 1942). An isolated, plate-like bone in the posteroventral part of A/I 4402 possibly represents the subopercle (Figs. 2, 3). The putative subopercle is about half as large as the opercle and has a trapezoidal shape. It is bounded by gently diverging dorsal and ventral confinements, and subparallel anterior and posterior margins. The posterior border is convex and longer than the anterior one. Dermal ornament of the bones of the operculogular series consists of tubercles. Enlarged tubercles are seen on the anterodorsal part of the opercle, the anterior part of the subopercle, and the gulars.

Circumorbitals, nasals.—Immediately anterior to the right preopercle and the postorbital plate of the maxilla are several anamestic bones, the suborbitals (Figs. 2–4). There is one large upper suborbital and four additional, smaller, lower suborbitals, all of which appear to be preserved nearly in situ. The upper suborbital is roughly four-sided, with rounded corners. This bone is bounded by long dorsal and ventral margins, which run subparallel, a straight posteroventral border, and a deeply convex anterior confinement. The four lower suborbitals have polygonal outlines. All suborbitals are ornamented with tubercles, although each of them is marked by narrow unornamented regions along some of their margins.

Anterior to the right maxilla and suborbitals are several, serially arranged bones belonging to the right infraorbital series. The most posterior of these elements is identified as the jugal (Figs. 2–4). This bone is somewhat higher than long and roughly four-sided. It is confined by short, straight dorsal and anteroventral margins, a long, convex posterior border, and a short, concave anterodorsal margin. The infraorbital sensory canal traverses the jugal nearer to its anterodorsal margin than to its posterior border. The area caudal to the sensory canal is ornamented with coarse tubercles, whereas the part anterior to it is smooth. An elongate, canal-bearing element, located anteroventral to the jugal, probably belongs to the infraorbital series (Fig. 4.1). In vivo, this element may have been situated dorsal to the jugal. The lateral surface of this infraorbital bone is divided into an unornamented dorsal (originally anterior?) part and a ventral (originally posterior?) portion ornamented with large tubercles. The ventral part is pierced by a sensory canal. Anteroventral to the infraorbital bone is a much larger, rostrocaudally elongate element: the lachrymal (Figs. 2, 4). The subquadrangular lachrymal is bounded by long dorsal and ventral margins, and short anterior and posterior borders. Caudally, the lachrymal still articulates with the anterior process of the maxillary bone. The lachrymal lacks ornamentation, but a distinct longitudinal crest on its lateral surface possibly indicates the course of the infraorbital sensory canal. Several minute teeth are developed on the ventral surface of the lachrymal, similar to those on the anterior process of the maxilla. Anterodorsal to the lachrymal is a smaller, slightly dislocated bone, which we interpret as the antorbital (Fig. 4.1). The antorbital is plate-like and its lateral surface, now facing anterodorsally, is covered with coarse tubercles. The medial surface is smooth and marked by a thickened portion along the now posteroventrally located margin, which contains a sensory canal. Two small, thin bones dorsal to the lachrymal may pertain to elements of the sclerotic ring (Fig. 4.1). The two bones still articulate with each other. Both show an elongate, somewhat rectangular outline. Their lateral surface is mostly smooth, but marked by a single line of small but distinct tubercles along their dorsal margin. In the rostral area, there is a single, plate-like element, interpreted as the right nasal, which is traversed by a sensory canal, the supraorbital canal (Fig. 4.1). The trapezoidal nasal is divided into two portions: a stout posterior part, covered with coarse tubercles, and a thinner anterior part, which is smooth.

Dermal skull roof.—A patch of articulated bones in the caudal region of part a (Fig. 2) is tentatively interpreted as the posteriormost part of the dermal cranial roof. Two symmetrically arranged fragments, situated posterolaterally on the putative dermal skull roof, show distinct ornamentation composed of mainly anteroposteriorly aligned striae and some tubercles along the posterior border. These two bone fragments are identified as the caudal portions of the dermopterotics. Two much smaller elements, wedged between the dermopterotics, possibly correspond to the parietals. Posterior to the left dermopterotic are several smaller, plate-like bones, a large lateral and about two smaller, medial elements, which would correspond to the extrascapulars. The parietal and extrascapulars are covered with tubercles.

Hyoid and branchial arches.—Several scattered, elongate ossifications in the anterior region of A/I 4402 correspond to bones of the hyoid and branchial arches. A fragment of the right hyomandibula is preserved between the right supracleithrum and the right posttemporal (Figs. 2, 3). The hyomandibula consists of an anterior and a posteroventral shank that meet in an obtuse angle. The most rostral and most ventral extremities of this bone are missing. An opercular process is not developed, but the posterodorsal margin of the angled portion bears a very low, blade-like protrusion. An elongate, triangular element

https://doi.org/10.1017/jpa.2019.18 Published online by Cambridge University Press

attached to the upper part of the lateral surface of the anterior shank corresponds to the dermohyal. The dermohyal is ornamented with tuberlces (Fig. 3.3). The ceratohyal, preserved dorsal to the left mandible (Fig. 2), is an elongate, plate-like bone with an hourglass-shaped outline. Its anterior margin runs perpendicular to the longitudinal axis of the bone, whereas the posterior termination is inclined. A weak, sigmoid longitudinal groove is observed on the ceratohyal, corresponding to the groove for the afferent hyoid artery (cf., Nielsen, 1942, fig. 43).

Several rod-like bones preserved predominantly in the cranial area of the fossil belong to the gill arches. Two elongate elements, lying on the branchiostegal rays (A/I 4402b; Fig. 3), are dorsoventrally compressed and show a furrow along their longitudinal axis. Their morphology suggests that they are ceratobranchials. A shorter element with a similar morphology, possibly an epibranchial, is situated rostral to the left pectoral fin (Fig. 2).

Shoulder girdle.—Most elements of the dermal shoulder are disarticulated, with those from the right side of the shoulder girdle now located close to the right pectoral fin, whereas the bones from the left side are found near the left pectoral fin (Figs. 2, 3). Both posttemporals are present. The large posttemporal consists of a broad, dorsally convex external plate, and a medioventral process. The plate-like part has a roughly triangular outline, being confined by a long, convex posteromedial border, a slightly shorter, straight lateral margin, and a short, straight anterior border. The transitions between these margins are rounded. The dorsal surface is covered with tubercles, which gain in size towards the broad anterior end of the bone. The tubercles are, to some degree, anteroposteriorly aligned and may occasionally change into short, longitudinal striae. The canal for the lateral line can be traced near the lateral margin. The ventral process is incompletely preserved, but its proximal portion is seen on the left posttemporal in A/I 4402a, and the right one in A/I 4402b (Fig. 3.3). The medial process issues in proximity to the lateral margin of the plate-like part. The supracleithrum is a dorsoventrally broad, plate-like bone. It is bounded by a long and slightly convex posterior margin, a long, gently concave anterior border, and more or less convex dorsal and ventral borders. A pore line on the external side of both supracleithra, running from the middle of the posterior confinement of the bone and traversing obliquely in anterodorsal direction, indicates the course of the lateral line canal. The canal left the bone near its dorsal end. It traversed the ossification center of the supracleithrum, situated on the longitudinal axis of the bone, close to its dorsal end. The external surface of the supracleithrum is convex and ornamented with round to oblong tubercles, arranged in lines radiating from the ossification center.

The cleithrum is bounded by a straight ventral border, a long, concave anterodorsal margin, and a long, sigmoid posterior border, which is convex dorsally and concave in its ventral portion (the concavity indicating the place of insertion of the pectoral fin). The anterior branch of the cleithrum, now directed caudally, is slightly shorter and more slender than the upper one. The external surface of the cleithrum is distinctly convex. A few coarse tubercles are visible on the ventral edge of the lower division of the cleithrum (Fig. 3), but the ornamentation of the remaining areas is not preserved. The endochondral shoulder girdle is not detectable. Whereas the right clavicle is preserved nearly in situ (Fig. 2), the left one is found next to the anterior end of the left cleithrum (Figs. 2, 3). The clavicle has a triangular outline in dorsoventral aspect, with long and straight medial and lateral margins, and a short, straight posterior border. The external (ventral) surface is convex and ornamented with tubercles, which increase in coarseness towards the broad caudal end of the bone.

Paired fins.—The exoskeletal parts of both pectoral fins are preserved in situ (Figs. 2, 3). The left pectoral fin is distally more complete than the right one. The fin is fairly large, three-sided and, based on the manner of preservation, was oriented horizontally in the living animal. It has a long, convex anterior border and a nearly straight basal margin. About 27 fin rays are in the right pectoral fin (cast of A/I 4402a). Ornamentation of the fin rays consists of a few longitudinal ridges. All lepidotrichia are segmented, with the most basal segment always distinctly longer than the following ones. The basal segments are longer in the ventral hemitrichia (A/I 4402b; Fig. 3) than they are in the dorsal hemitrichia (A/I 4402a; Fig. 2). The leading edge of the pectoral fin is made of several rays. Bifurcation (at least one or two times each) is observed in the distal part of the fin rays, both on the lepidotrichia terminating at the anterior fin margin (except for the first three rays) and the lepidotrichia terminating at the posterior fin margin. The anterior margin of the fin is armed with two long basal fulcra (A/I 4402b) and numerous, distally adjoining, smaller fringing fulcra. The series of fringing fulcra is seemingly interrupted by terminal lepidotrichia segments (see Fig. 2.3), thus exhibiting Pattern B of Arratia (2009). A slender, scaled lobe is developed at the base of the right pectoral fin (A/I 4402a). The fin endoskeleton is poorly preserved.

Only the left pelvic fin is preserved and seen in situ in A/I 4402a (Fig. 2). It is mostly complete, but the pelvic girdle is not visible. The fin has a triangular shape, being confined by gently convex anterior and posterior borders, and a relatively long, straight basal margin (nearly as long as that of the pectoral fin). About 23 lepidotrichia are counted (cast of A/I 4402a). All lepidotrichia are composed of short segments, with the basal segment of each fin ray not being significantly longer than the following ones. As far as can be seen, the seventh fin ray and all the posteriorly following ones terminating at the caudal margin of the fin are distally bifurcated at least once. The leading edge of the fin is formed by six unbranched rays, which become gradually longer (Fig. 2.2). They are lined with an incompletely preserved series of fringing fulcra (probably showing Pattern B of Arratia, 2009).

Unpaired fins.—The unpaired fins are incompletely preserved and shifted from their in vivo positions. A patch of lepidotrichia and some pterygiophores located in the posterior part of A/I 4402a are tentatively interpreted as belonging to the anal fin and its endoskeletal support (Fig. 2). Our interpretation is based on the proximity of these elements to a large patch of scales (now located posterior to the pelvic fin) that probably comes from the ventral body region. Sixteen anal fin rays are preserved, each of which is made up of several short segments. Branching is not observed, probably related to the incomplete preservation of the fin. Very few fringing fulcra are visible along the leading margin of the fin. Several lepidotrichia located between the pectoral and pelvic fins probably pertain to the dorsal fin (Figs. 2, 3). Their segmentation pattern is similar to that of the putative anal fin.

https://doi.org/10.1017/jpa.2019.18 Published online by Cambridge University Press

A large patch of lepidotrichia preserved near the anal fin is identified as the ventral lobe of the caudal fin (A/I 4402a, Fig. 2) due to the greater stoutness of the fin rays compared to those of the other fins. The distal parts of the ventral caudal lobe are missing. Up to 20 lepidotrichia are preserved, all of which consist of several short segments. The basal segment of each lepidotrichium is always the longest one. At least the five most posterior fin rays are distally branched either once or twice. The leading edge of the ventral caudal lobe is made of at least eight gradually longer rays, which are covered with fringing fulcra of Arratia's (2009) Pattern B. Additionally, there are two basal fulcra. A further patch of lepidotrichia anterolateral to the ventral caudal lobe possibly belongs to dorsal lobe of the caudal fin (A/I 4402a, Fig. 2). It is composed of seven very fine fin rays, all of which are made of numerous short segments and that are dichotomized up to three times distally.

Squamation.—The trunk of A/I 4402 (Figs. 2, 3) was covered with mostly rhombic scales arranged in oblique vertical rows. On some isolated rhombic scales (Fig. 2.3), a small dorsal peg is visible (peg-and-socket articulation). Scales from the dorsal/ventral body portions are much longer than deep and those on the flanks less so (as seen on the large articulated patch of scales between the pelvic fin and the presumed anal fin). On some scales, the ornamentation of the free field consists of rostrocaudally oriented striae (Fig. 2.4). Scales preserved at the base of the caudal fin show smooth free fields. The posterior margin of the rhombic scales is either denticulated or straight (Fig. 2.3, 2.4). On the medial side, the scales are thickened centrally along their dorsoventral axis.

Several specialized scales are observed. An accumulation of broad, ellipsoid ridge scales is found just anterior to the left pectoral fin (Figs. 2, 3). These ridge scales, which may have been associated with the nearby dorsal fin, are pointed at their posterior end and characterized by a convex external surface. Further, more lanceolate ridge scales are found near the base of the putative anal fin and the area between the two patches of caudal fin rays (Fig. 2). The lanceolate ridge scales may have been associated with the anal fin in vivo. Ridge scales were seemingly only regionally developed along the ventral midline: a section of the ventral midline, preserved between the pectoral fins and the left pelvic fin (A/I 4402a, Fig. 2), clearly lacks ridge scales. At least one large, unpaired basal fulcrum (sensu Patterson, 1982) is preserved close to the putative patch of dorsal caudal fin rays (Fig. 2). This fulcrum, which belonged to the anterior margin of the upper caudal lobe, has an elongate habitus, with a pointed posterior end, and bifid, acute anterior terminations.

Etymology.—The species name *nevadanus* refers to the US state of Nevada.

Remarks.—The morphology of PIMUZ A/I 4402 agrees with that of the Early–Middle Triassic *Pteronisculus* White, 1933. A key character of A/I 4402 is the extension of the dentigerous lachrymal (= 'lacrimo-maxillary' of Nielsen, 1942) to the oral margin, considered an autapomorphy of *Pteronisculus* (Xu et al., 2014). Other features supporting the attribution of A/I 4402 to *Pteronisculus* are: (1) morphology of the lower jaw (e.g., relative size of the coronoids and prearticular, number of coronoids); (2) shape, reduced ornamentation, and large size of the opercle and the much smaller subopercle, as well as the number of gulars and branchiostegals; (3) presence of a posttemporal (= 'suprascapular' of Nielsen, 1942) with a mediolaterally expanded rostral margin and the large, broad supracleithrum; (4) the large size of the pectoral fin and the relatively smaller pelvic fin, as well as the number of lepidotrichia of the paired fins and their segmentation pattern (pectoral fin with long basal lepidotrichial segments, pelvic fin composed of short fin ray units throughout); and (5) the squamation (e.g., general ornamentation pattern, presence of smooth scales in the posterior body portion, restricted distribution of specialized ridge scales). Although several of these characters are also present in other 'palaeoniscoids' (e.g., Aldinger, 1937; Nielsen, 1942; Schaeffer, 1952; Müller, 1962), their combined occurrence in the Nevada specimen supports its inclusion in *Pteronisculus*. The estimated total length of A/I 4402 (180–200 mm) is comparable to that of other species, such as *P. cicatrosus* White, 1933, *P. arcticus*, or *P. stensioi*.

Reported occurrences of *Pteronisculus* are listed in Table 1. At least 11 species have been documented from geographically distant, marine Early Triassic localities (e.g., Stensiö, 1921, 1932; Nielsen, 1942; Lehman, 1952; this study), and one species has recently been described from the Middle Triassic (Anisian) Luoping Biota of Yunnan Province, China (Xu et al., 2014). Xu et al. (2014) mention the occurrence of *Pteronisculus* in the Middle Triassic of Spitsbergen, which is erroneous (see Stensiö, 1921; Kogan and Romano, 2016b). Occurrences of this taxon in Early Triassic marine strata of Alberta and British Columbia, Canada (*P.*? *laetus* [Lambe, 1916]; *Pteronisculus* sp.; Gardiner, 1966; Schaeffer and Mangus, 1976), and in Lopingian (late Permian) freshwater deposits of South Africa (*P.*? *meiringi* Gardiner and Jubb, 1975) are disputed (Bender, 2004; Neuman, 2015). The contribution of the lachrymal to the oral margin was neither described in the Canadian nor the South African material. Specimen A/I 4402 provides the first, unequivocal evidence for the presence of *Pteronisculus* in the eastern, low-latitudinal Panthalassa.

Species of *Pteronisculus* are distinguished, chiefly, by the relative length of the postorbital portion of the maxilla, the number and arrangement of the suborbitals, and the ornamentation pattern of the scales and dermal bones (e.g., Nielsen, 1942; Lehman, 1952; Xu et al., 2014). Erection of a new species for A/I 4402, *Pteronisculus nevadanus* n. sp., is justified due to a unique combination of characters (see differential diagnosis). The present study supports the view of Xu et al. (2014) that the premaxilla is absent in *Pteronisculus*. A (paired) premaxilla has only been described in *P. stensioi* (Nielsen, 1942), but with doubt.

Family Ptycholepidae Brough, 1939
Genus *Ardoreosomus* new genus

Type species.—*Ardoreosomus occidentalis* n. gen. n. sp., by monotypy.

Diagnosis.—As for the type species by monotypy.

Etymology.—The name comprises two words, *ardores* (Latin), meaning 'tropics,' reflecting the low-latitude position of

https://doi.org/10.1017/jpa.2019.18 Published online by Cambridge University Press

Nevada during the Early Triassic, and *somus* (σῶμα, ancient Greek, latinized), meaning 'body.'

Remarks.—*Ardoreosomus* n. gen. is referred to Ptycholepidae Brough, 1939 mainly due to the arrangement of the fins, notably the dorsal fin. A new genus is warranted, among others, due to the more strongly angled hyomandibula, which lacks an elongate opercular process.

Ardoreosomus occidentalis new species
Figures 5, 6, 7.1

Holotype.—NMMNH P-57422 (Fig. 5) is preserved in a large nodule, the counterpart of which is missing. A silicone cast was produced for this study.

Diagnosis.—Mid-sized ptycholepid; hyomandibula with small opercular process (elongate process in *Ptycholepis*, *Boreosomus*, *Acrorhabdus*); angle between anterior and posteroventral hyomandibular shanks smaller than in *Ptycholepis*, *Boreosomus*, *Acrorhabdus*; numerous tooth plates dorsal to ectopterygoid and dermopalatine (as in *Acrorhabdus*, some *Boreosomus*, unlike *Ptycholepis*); anterior preopercular shank more rostrally inclined than in *Ptycholepis*, *Boreosomus*, *Chungkingichthys*, *Yuchoulepis*; opercle oblong (subquadrangular in *Yuchoulepis*); dentary and opercle with tubercles (striae in *Ptycholepis*, *Acrorhabdus*, *Chungkingichthys*, *Yuchoulepis*); dorsal fin inserting at the same vertical scale row as anal fin (dorsal fin situated several scale rows ahead of anal fin in *Ptycholepis*, *Boreosomus*, *Yuchoulepis*); anal fin closer to pelvic fins than caudal fin (closer to caudal fin in *Ptycholepis*, *Boreosomus*, *Yuchoulepis*); flank scales about as deep as long (similar to *Boreosomus*, *Chungkingichthys*, flank scales longer than deep in *Ptycholepis*, *Yuchoulepis*); enlarged pre-anal scales developed (absent in *Ptycholepis*, *Boreosomus*, *Chungkingichthys*, *Yuchoulepis*).

Occurrence.—From the lower Candelaria Formation (middle-upper Dienerian, Lower Triassic) of the eastern Candelaria Hills (Esmeralda County, Nevada, USA).

Description.—NMMNH P-57422 is largely complete, with an approximate standard length of 200–250 mm. Whereas most elements of the trunk are preserved in situ, the skull and shoulder girdle are disarticulated.

Jaws.—Only some skull bones of NMMNH P-57422 can be identified with certainty. Of the upper jaw, mainly the left palatoquadrate, with the impressions of its lingual dermal cover, as well as both maxillae are preserved. The left palatoquadrate (Figs. 5, 6.1) is a three-sided element, with a long, gently concave ventral margin, a short, convex posterior border, and a long anterodorsal margin, whose outline is obscured by a patch of scales. Whether an articular fossa for the basipterygoid process is developed or not can thus not be determined. The most posterior and most anteroventral portions of the palatoquadrate are both curved laterally. The pars quadrata of the palatoquadrate has a subtriangular outline, but its anterior margin is difficult to trace. The ventral part of the medial surface of the palatoquadrate was covered by at least two serially arranged bones, the ectopterygoid and dermopalatine (Figs. 5, 6.1). Their boundaries are imperfect. Dorsal to the ectopterygoid are the impressions of numerous, small polygonal plates of varying sizes, ('entopterygoid plates,' cf. *Acrorhabdus bertili* Stensiö, 1921). Unlike the adjacent scales, the 'entopterygoid plates' do not overlap each other, but rather form a mosaic cover on the lingual side of the palatoquadrate. Both maxillae are visible. The right maxilla is fragmentary, but evidently consisted of an elongate rostral process and a plate-like postorbital portion (Figs. 5, 6.2). The rostral process is incomplete anteriorly and was probably much longer in vivo (in comparison with the size of the palatoquadrate). A fragment of the postorbital plate of the left maxilla is seen posteroventral to the right maxilla. Its medial surface is marked by the imprint of the internal (horizontal) lamina. The ventral border of the postorbital blades of both maxillae are lined with numerous, minute, pointed teeth (Fig. 6), best visible on the silicone cast.

The complete, left branch of the lower jaw is located ventrally to the pectoral fin, and a fragment of the right lower jaw is preserved dorsal to the left one (Fig. 5). The lower jaw is composed of at least two bones: the large dentary anteriorly, and the much smaller angular posteriorly. Their mutual boundary is not well visible. The external surface of the left lower jaw is weathered, but the general outline is still visible. It has a long, sigmoid dorsal margin, which is concave anteriorly and weakly convex posteriorly. The long ventral confinement is partially obscured by the ceratohyal, but had a sigmoid shape as well. It is convex anteriorly and posteriorly, and concave in its middle segment. The posterior margin of the left lower jaw branch, formed by the angular bone, is short and convex. The rostral tip of the lower jaw is rounded and curved dorsally and medially. Minute teeth are preserved within the anterior half of the left dentary. The teeth are comparable in size to those on the maxilla. Traces of the mandibular sensory canal are observed on both branches of the lower jaw. The right lower jaw is covered with fine tubercles, which are arranged in anteroposteriorly running lines (silicone cast).

Preopercle and operculogular series.—Dorsal and posterior to the postorbital process of the right maxilla are two canal-bearing bone fragments, separated by a crack, which belong to the preopercle (Figs. 5, 6.2). The preopercle is angled, consisting of a rostrally expanded anterior shank and a short, slender posteroventral shank. The anterior shank is bounded by a rostral margin that appears to be deeply concave, and a convex posterodorsal border. Its ventral margin, bordering the maxilla, is not well preserved. The rostral and posterodorsal margins of the anterior shank taper in an elongate, pointed anterodorsal process ('neurocranial process;' Bürgin, 1992, p. 20). The suture between the preopercle and maxilla is damaged; however, when reconstructed, the posterodorsal border of the anterior preopercular shank and the dentigerous margin of the maxilla run nearly parallel to each other (Figs. 5, 6.2). The preopercular sensory canal pierces the bone through its anterodorsal process and traverses along the longitudinal axes of its two shanks.

A large, plate-like element located next to the right maxilla-preopercle complex corresponds to one of the opercles. The opercle has a slightly elongate, rhomboid outline, with gently convex margins and rounded corners. The bone is

https://doi.org/10.1017/jpa.2019.18 Published online by Cambridge University Press

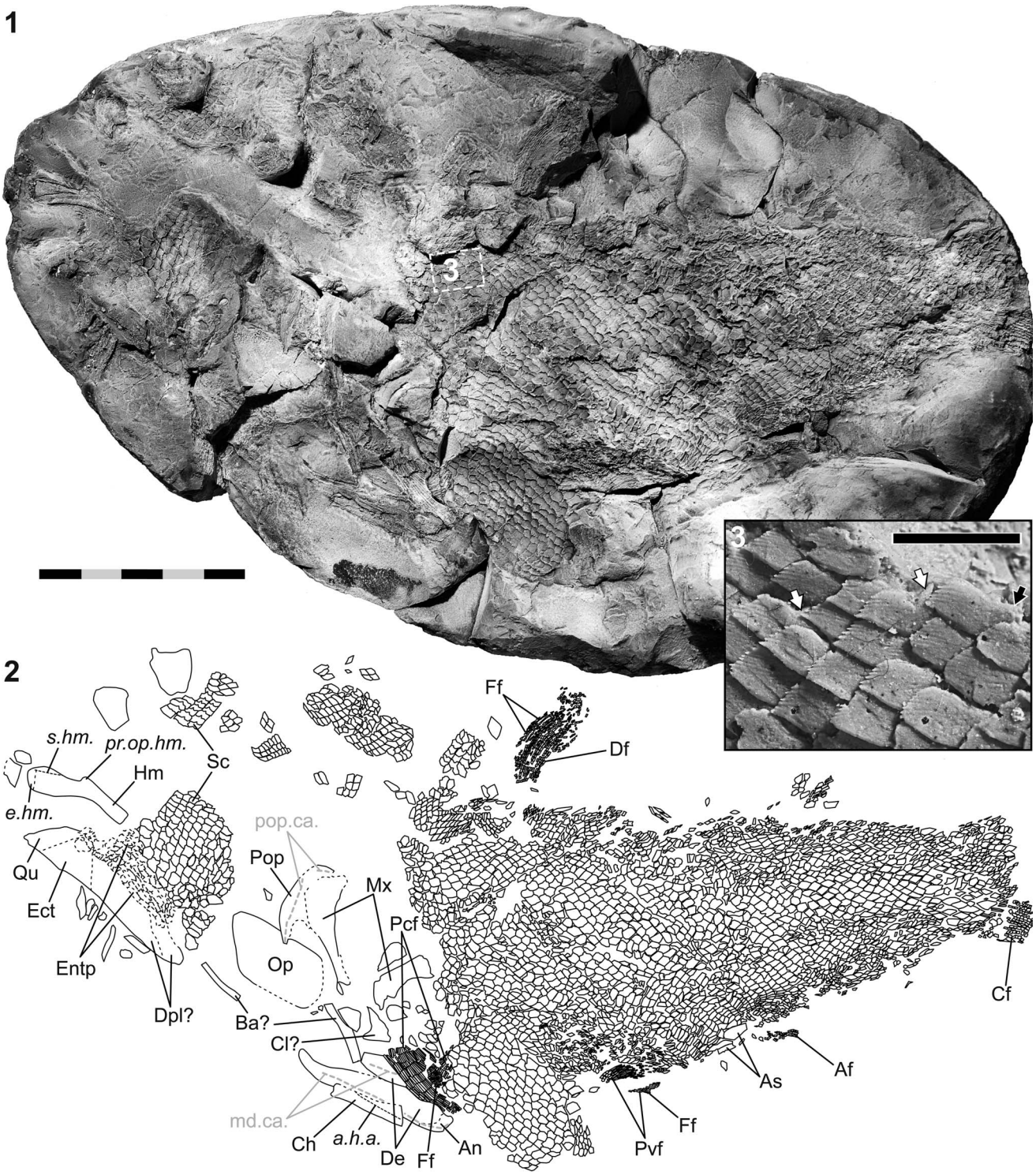

Figure 5. *Ardoreosomus occidentalis* n. gen. n. sp. from the middle-late Dienerian of the Candelaria Hills (Esmeralda County, Nevada, USA). (**1**) NMMNH P-57422 (holotype; enhanced with ammonium chloride); (**2**) schematic drawing of **5.1**, with and interpretations of bones; (**3**) close-up view of the squamation of the anterodorsal body portion of the silicone cast of NMMNH P-57422; white arrows point to the dorsal spine (peg-and-socket articulation). Anterior is left in **5.1** and **5.2**, and right in **5.3**. Scale bar measures 50 mm (total) in **5.1** and **5.2**, and 5 mm in **5.3**. Abbreviations: **Af**, anal fin (lepidotrichia); **a.h.a.**, groove for the afferent hyoid artery; **An**, angular; **As**, pre-anal scale; **Ba**, branchial arch element; **Cf**, caudal fin (lepidotrichia); **Ch**, ceratohyal; **Cl**, cleithrum; **De**, dentary; **Df**, dorsal fin (lepidotrichia); **Dpl**, dermopalatine; **e.hm.**, ossified cap of the hyomandibula ('epiphysis;' Stensiö, 1921; Nielsen, 1942); **Ect**, ectopterygoid; **Entp**, 'entopterygoid plates;' **Ff**, fringing fulcrum; **Hm**, hyomandibula; **md.ca.**, mandibular sensory canal; **Mx**, maxilla; **Op**, opercle; **Pcf**, pectoral fin (lepidotrichia); **Pop**, preopercle; **pop.ca.**, preopercular sensory canal; **pr.op.hm.**, processus opercularis hyomandibulae; **Pvf**, pelvic fin (lepidotrichia); **Qu**, quadrate; **Sc**, scale; **s.hm.**, sulcus for the truncus hyomandibularis of the facial nerve.

https://doi.org/10.1017/jpa.2019.18 Published online by Cambridge University Press

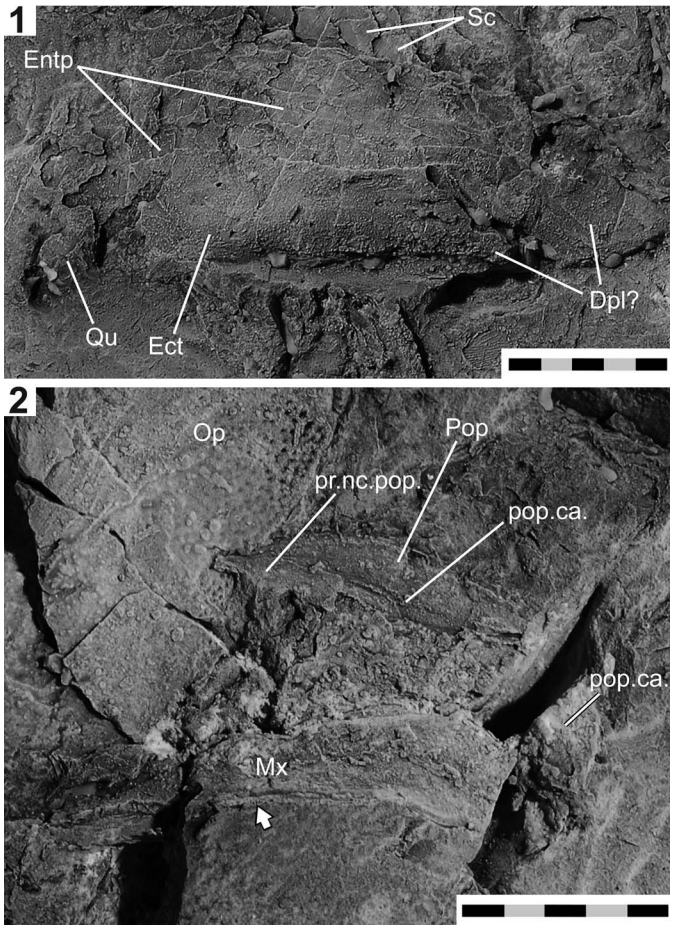

Figure 6. *Ardoreosomus occidentalis* n. gen. n. sp. from the middle-late Dienerian of the Candelaria Hills (Esmeralda County, Nevada, USA). (**1**) Close-up photograph of the left palatoquadrate of NMMNH P-57422 in medial aspect, showing imprints of its dermal bones; (**2**) close-up photograph of the right maxilla-preopercle-complex of NMMNH P-57422. The white arrow in **6.2** points to imprints of minute teeth along the ventral margin of the maxilla. Scale bar measures 10 mm (total) in **6.1** and **6.2**. Abbreviations: **Dpl**, dermopalatine; **Ect**, ectopterygoid; **Entp**, 'entopterygoid plates' (Stensiö, 1921); **Mx**, maxilla; **Op**, opercle; **Pop**, preopercle; **pop.ca.**, preopercular sensory canal; **pr.nc.pop.**, anterodorsal process of the preopercle ('neurocranial process;' Bürgin, 1992); **Qu**, quadrate; **Sc**, scale.

seen from its concave medial side. In the now rostrally and dorsally located parts of the opercle, the bone has partially weathered and the impressions of the ornamentation of the external surface are visible (Fig. 6.2). In these regions, the ornamentation consists of tubercles, which are coarse, pointed, and inclined in the same direction. Judging from the orientation of the apices of the tubercles (best seen on the cast), the now anteriorly facing margin corresponds to the posteroventral border of the opercle. Within the anterodorsal part of the bone, now located posteriorly and ventrally, several concentric growth lines are visible.

Hyoid and branchial arches.—One of the hyomandibulae is preserved in the anterior region of the fossil (Figs. 5, 7.1). It is composed of an anterior and a posteroventral shank, which meet in an obtuse angle (~155°). A small, dorsally directed processus opercularis is developed at the back of the angled portion of this bone. The dorsoventral width of the anterior shank increases rostrad. The width of the posteroventral ramus is much smaller than that of the anterior shank and remains constant throughout its length. Within the upper part of the anterior shank, there is a distinct groove, running in anteroposterior direction and merging with the upper margin of the anterior ramus just in front of the opercular process. This sulcus may have been associated with the truncus hyomandibularis of the facial nerve (VII), implying that the element in question is the right hyomandibula in medial view. The rostral end of the bone is capped by cancellous bone ('epiphysis;' Stensiö, 1921; Nielsen, 1942). The left ceratohyal is preserved beneath the left lower jaw (Fig. 5). This elongate, platelike bone is about half as long as the lower jaw, and bounded by four confinements: a short, straight anterior border, a short posterior margin, a long, slightly S-curved ventral border, and a gently concave dorsal margin. The anterior, dorsal, and ventral borders meet orthogonally, whereas the posterior border is inclined. A groove on the lateral side of the ceratohyal indicates the course of the afferent hyoid artery. A few disarticulated, rod-like bones that are distributed in the anterior region of P-57422 possibly represent elements of the branchial arches.

Shoulder girdle.—Most elements of the dermal and endochondral shoulder girdle are not preserved or not identifiable. However, a small bone fragment found close to the base of the right pectoral fin may pertain to either the right cleithrum or the right clavicle (Fig. 5). It is ornamented with tubercles, which are particularly large along the straight ventral margin.

Paired fins.—Of both pectoral fins, only the lepidotrichia are preserved, with those of the left pectoral fin lying on top of the right one (Fig. 5). The fin rays of the right pectoral fin are oriented perpendicularly to those of the left one. There are ~16 lepidotrichia in the left pectoral fin, but the original number was higher. With the exception of the first one or two rays, all lepidotrichia are composed of short segments distally, and at least some of them dichotomize. The leading edge of the right pectoral fin is armed with fairly large fringing fulcra (apparently Pattern C; Arratia, 2009). Both pelvic fins are in situ, but the pelvic girdle is covered by the scales. The pelvic fins are small and located halfway between the pectoral and the anal fins (Fig. 5). The right pelvic fin is more complete than the left one. The fin rays ramify distally and are made up of many short segments. We count about eight to nine fin rays in each of the two ventral fins. A few fringing fulcra line the leading edge of the left fin.

Unpaired fins.—The anal fin is located closer to the pelvic fins than to the caudal fin (Fig. 5). Only the basal portions of a few fin rays are visible, each consisting of short segments. Fulcra are not visible and the pterygiophores of the anal fin are not exposed. Differing from most coeval actinopterygians, the dorsal fin of P-57422 is not situated at the level of the anal fin, but rather in front of the pelvic fins (Fig. 5). Nevertheless, the dorsal fin inserts at about the same scale row as the anal fin. Considering that the other unpaired fins and the pelvic fins are preserved in situ, despite their fragmentary preservation, it is assumed that the dorsal fin is also still in situ. Only ~12 lepidotrichia of the dorsal fin are preserved, but the original number was higher. All fin rays are evenly segmented, distal bifurcation is not evident. The leading edge of the dorsal fin is equipped with fringing fulcra (probably Pattern C; Arratia, 2009). Regarding the caudal fin, only the basal parts of ~11 lepidotrichia of the ventral lobe are preserved (Fig. 5). The fin rays of the lower caudal lobe are

https://doi.org/10.1017/jpa.2019.18 Published online by Cambridge University Press

composed of numerous segments, whereas the most basal segment of each fin ray is longer than the distally following ones, which are box-shaped (i.e., with a nearly quadratic outline in lateral view). Fulcra are visible along the ventral margin.

Squamation.—The trunk is covered with rhombic scales, arranged in inclined rows (Fig. 5). The squamation is incomplete, but ~48–50 vertical scale rows are counted on the flank between the anterior and caudal ends of the trunk. Whereas the scales on the lateral side of the body are about equally high as long, those occupying a more dorsal or ventral position are distinctly longer than high. The hind margin of the scales is denticulated (Fig. 5.3). Ornamentation of the free field consists of oblique, anteroposteriorly running striae (strongly to weakly developed), which coalesce with the denticles. The striae occasionally show an anastomosing pattern. The anterior part of each scale, which is laterally covered by one or two preceding scales, is wide. A well-developed dorsal peg, which fits into a groove on the medial side of the adjacent scale (peg-and-socket articulation), and an anterodorsal process are only developed on the scales of the anterior body portion (Fig. 5.3), while both are absent on the scales of the posterior trunk region. Anterior to the anal fin, about four enlarged, pre-anal scales are observed, which surrounded the anus in vivo (Fig. 5). In addition, at least two scales covered with strong striae occur next to the pelvic fins. The lateral line cannot be traced with certainty in the scales.

Etymology.—The species name refers to the West (Occident), from Latin *occidens*.

Materials.—MNHN.F.MAE 6 (*Boreosomus gillioti* [Priem, 1924]), PIMUZ T 1008, T 1378, T 2874 (*Ptycholepis barboi* Bassani, 1886; Bürgin, 1992).

Remarks.—A striking feature of NMMNH P-57422 is the far forward position of the dorsal fin, situated slightly anterior to the pelvic fins. This is a rare condition among fusiform early actinopterygians and typical, for instance, for the Mesozoic families Ptycholepidae Brough, 1939 and Platysiagidae Brough, 1939, which according to Mutter (2011) are closely related (but see Wen et al., 2019). We regard the inclusion of P-57422 in Platysiagidae as less likely due to the large size of the Nevada specimen (platysiagids: ≤8 cm), the more anterior position of the dorsal fin (this fin is located at the level of the posterior end of the ventral fins in platysiagids), and the presence of an anterodorsal process ('neurocranial process;' Bürgin, 1992) on the preopercle, absent in platysiagids (Stensiö, 1932; Brough, 1939; Nybelin, 1977; Bürgin, 1992; Neuman and Mutter, 2005; Wen et al., 2019). In contrast, the morphology of P-57422 agrees with that of Ptycholepidae (= Boreosomidae Gardiner, 1967; Chungkingichthyidae Su, 1974; cf., Mutter, 2011). Following Mutter (2011), this family encompasses *Ptycholepis* Agassiz, 1832 (Middle Triassic–Early Jurassic; Mutter, 2011), *Boreosomus* Stensiö, 1921 (= *Diaphorognathus* Brough, 1933; Early Triassic, Nielsen, 1942; Lehman, 1952), *Acrorhabdus* Stensiö, 1921 (Early Triassic), *Chungkingichthys* Su, 1974 (Early Triassic, for the age see Xu et al., 2015 and references therein), and *Yuchoulepis* Su, 1974 (Early Triassic; Xu et al., 2015). We agree with Tintori et al. (2016) that the Triassic material of *Ptycholepis* requires critical revision.

Affinity of P-57422 to the Triassic–Early Jurassic Ptycholepidae is indicated by the combined presence of the following traits: the constellation of the fins (particularly the far forward position of the dorsal fin) and their segmentation/branching patterns, cranial features (e.g., anterodorsal process of the preopercle, large opercle, cleaver-shaped maxilla, slender lower jaw, absence of a foramen in the hyomandibula for the facial nerve), the number of transversal scale rows (usually ~41–59; Nielsen, 1942; Su, 1974; Schaeffer et al., 1975; Bürgin, 1992), and scale morphology. Specimen NMMNH P-77357 from Crittenden Springs (Elko County, Nevada), described by Romano et al. (2017), may be referred to Ptycholepidae as well based on the relative position of the dorsal fin and the fin segmentation pattern.

The presence of numerous small dermal elements ('entopterygoid plates;' Stensiö, 1921) dorsal to the ectopterygoid and dermopalatine of P-57422 resembles the condition in *Acrorhabdus bertili* Stensiö, 1921, but in *A. bertili* an additional, larger bone (entopterygoid) is present rostrally. In other ptycholepids (*Boreosomus*, *Ptycholepis*), there is usually either a single, large entopterygoid or no dermal element at all dorsal to the ectopterygoid (Stensiö, 1921; Brough, 1939; Nielsen, 1942; Lehman, 1952; Bürgin, 1992). However, Véran (1988) indicated denticulated plates in a specimen of *Boreosomus reuterskioldi* Stensiö, 1921 (also see Véran, 1996). Such tooth plates, sometimes referred to as the 'dermometapterygoid(s)' because they cover the metapterygoid portion of the palatoquadrate, were described in many fossil actinopterygians and in *Amia* Linnaeus, 1766 and *Polypterus* St. Hilaire, 1802 and these plates often fuse ontogenetically with either the metapterygoid, the entopterygoid, or the ectopterygoid (Gardiner, 1984; Arratia and Schultze, 1991). Another common feature of P-57422 and ptycholepids is the lack of a foramen for the cranial nerve (VII) in the hyomandibula (Stensiö, 1921; Nielsen, 1942), otherwise present in many actinopterygians. The sulcus on the medial surface of the anterior hyomandibular shank of P-57422 suggests that the facial nerve traversed this bone above it, just in front of the opercular process. Nielsen (1942) already assumed that such was the case in *Boreosomus*. In P-57422, ptycholepids, and other ray-fins (e.g., *Acipenser* Linnaeus, 1758; Hilton et al., 2011), the hyomandibula shows a cap of cancellous bone ('epiphysis' in Stensiö, 1921, p. 226; Nielsen, 1942, p. 345).

Cranial differences between P-57422 and other Ptycholepidae concern the angle between the hyomandibular shanks, and the size of the processus opercularis (Fig. 7). Whereas the opercular process is very small in P-57422, it is elongate in *Acrorhabdus*, *Boreosomus*, and *Ptycholepis* (Stensiö, 1921; Brough, 1939; Nielsen, 1942; Schaeffer et al., 1975; Bürgin, 1992). Moreover, while the two shanks of the hyomandibula meet at an angle of ~155° in the Nevada specimen, this angle approaches ~180° in other ptycholepids (Fig. 7.2; Stensiö, 1921; Brough, 1939; Nielsen, 1942; Lehman, 1952; Schaeffer et al., 1975; Bürgin, 1992). The more oblique suspensorium of P-57422 is also reflected in the less obtuse angle between the two preopercular shanks, compared to other ptycholepids (Nielsen, 1942; Su, 1974; Schaeffer et al., 1975;

https://doi.org/10.1017/jpa.2019.18 Published online by Cambridge University Press

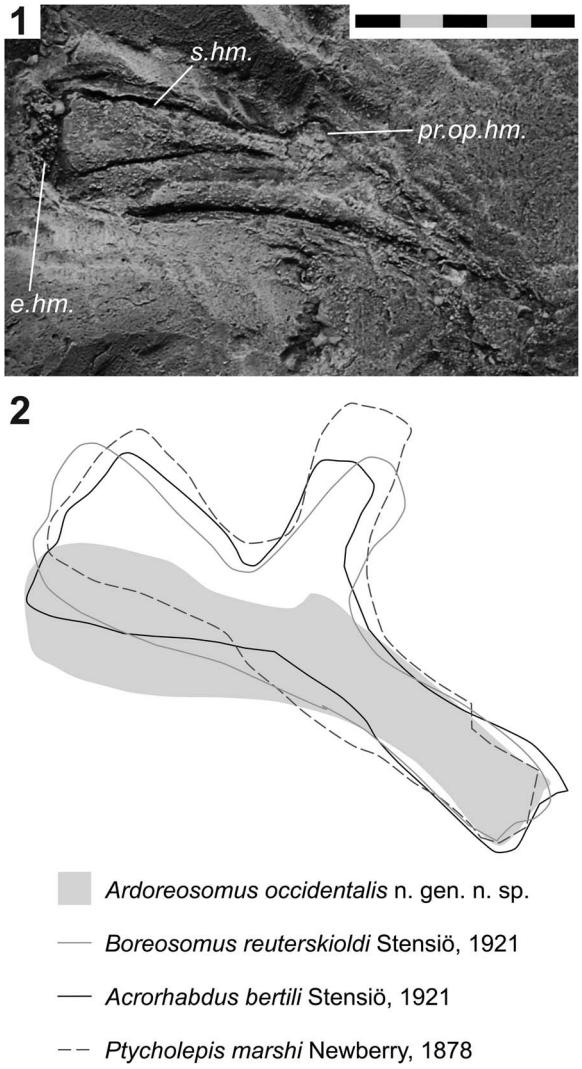

Figure 7. Hyomandibular shape in Ptycholepidae Brough, 1939. (**1**) Close-up of the right hyomandibula of NMMNH P-57422 (*Ardoreosomus occidentalis* n. gen. n. sp.) from the middle-late Dienerian of the Candelaria Hills (Esmeralda County, Nevada, USA); (**2**) comparisons of the shape of the hyomandibula between different members of Ptycholepidae Brough, 1939: *A. occidentalis* n. gen. n. sp. from the Candelaria Hills (NMMNH P-57422; holotype), *Boreosomus reuterskioldi* Stensiö, 1921 from the Smithian of Spitsbergen (Svalbard, Norway; Véran, 1988, pl. 2a), *Acrorhabdus bertili* Stensiö, 1921 from the Smithian of Spitsbergen (PMU P.174, Stensiö, 1921, pl. 31, fig. 1), *Ptycholepis marshi* Newberry, 1878 from the Late Triassic of the eastern USA (NMNH 21289; Schaeffer et al., 1975, fig. 3). Scale bar in **7.1** is 10 mm (total). Outlines of the hyomandibulae in **7.2** are not to scale. Hyomanibulae are aligned so that their posteroventral shanks run parallel. Abbreviations: **e.hm.**, ossified cap of the hyomandibula ('epiphysis;' Stensiö, 1921; Nielsen, 1942); **pr.op.hm.**, processus opercularis hyomandibulae; **s.hm.**, sulcus for the truncus hyomandibularis of the facial nerve.

Bürgin, 1992). There are also postcranial differences. Above all is the relative position of the anal fin, which is located nearer to the ventral fins than the caudal fin in P-57422, whereas in other ptycholepids the anal fin is situated closer to the tail fin (Nielsen, 1942; Lehman, 1952; Su, 1974; Bürgin, 1992). In addition, the anal and dorsal fins insert at approximately the same scale row in P-57422, whereas in *Boreosomus*, *Ptycholepis*, and *Yuchoulepis* the two fins insert several rows apart (Brough, 1939; Nielsen, 1949; Lehman, 1952; Su, 1974; Schaeffer et al., 1975; Bürgin, 1992; Mutter, 2011). Furthermore, specimen P-57422 possesses enlarged pre-anal scales, which were not described in any ptycholepid. Although Schaeffer et al. (1975) show an enlarged pre-anal scale in their reconstruction of *Ptycholepis marshi* Newberry, 1878, its presence cannot be verified based on the description or depicted specimens. Further differences between P-57422 and most Ptycholepidae concern the dermal ornament. In P-57422, the ornamentation of the opercle and dentary consists of tubercles that are frequently aligned anteroposteriorly. In most ptycholepids (*Acrorhabdus*, *Ptycholepis*, *Chungkingichthys*, *Yuchoulepis*), these bones are covered with rostrocaudally directed striae (Stensiö, 1921; Su, 1974, 1993; Schaeffer et al., 1975; Bürgin, 1992). Opercles ornamented with tubercles have been described in some specimens referred to *Boreosomus* (Stensiö, 1921; Lehman, 1952), although in other individuals these bones show longitudinal striae, in the typical ptycholepid fashion (Nielsen, 1942; Lehman, 1952; Ørvig, 1978).

Specimen P-57422 resembles *Boreosomus* and *Chungkingichthys* in having nearly quadrangular flank scales, as opposed to *Ptycholepis* and *Yuchoulepis*, which have elongate, low flank scales (Nielsen, 1942; Lehman, 1952; Su, 1974; Bürgin, 1992; Schaeffer et al., 1975). In MNHN.F.MAE 6 (*Boreosomus gillioti*), the anterior flank scales are deeper than long, suggesting some variation in this character. The scale ornamentation of P-57422 is similar to ptycholepids. Although scale ornamentation has been used to characterize species (e.g., Stensiö, 1921; Bürgin, 1992), its utility for taxonomy remains disputable—at least for some actinopterygians. Nielsen (1942) emphasized high intraspecific variation in *Boreosomus*.

In conclusion, the anatomy of P-57422 resembles that of the Ptycholepidae (sensu Mutter, 2011) for the most part, and it is thus referred to this family. However, specimen P-57422 differs from all other members of Ptycholepidae in four key features: (1) the more oblique suspensorium (evidenced by the shape of the hyomandibula and preopercle), (2) absence of an elongate opercular process on the hyomandibula, (3) presence of specialized pre-anal scales, and (4) the more anterior position of the anal fin. In light of these differences, a new genus and species is erected, *Ardoreosomus occidentalis* n. gen. n. sp. This new taxon further increases the diversity in preopercular morphology in Ptycholepidae (cf., Mickle, 2013).

The plesiomorphic anatomy of *Ardoreosomus* n. gen. suggests that some neopterygian-like characters of ptycholepids (e.g., presence of an opercular process, vertical jaw suspension) evolved within this clade—convergent to neopterygians. This view agrees with traditional systematic hypotheses (Aldinger, 1937; Nielsen, 1942; Bürgin, 1992) and is supported by cladistic analyses (e.g., Véran, 1988; Mickle, 2015; Giles et al., 2017), in which *Boreosomus* is resolved outside of Neopterygii. Brough (1936) suggested that the similarities between Triassic Neopterygii and other, more basal actinopterygians (his non-monophyletic 'Subholostei') are the result of convergent evolution—a hypothesis that could explain the mosaic distribution (e.g., López-Arbarello et al., 2016) of neopterygian characters in some Triassic actinopterygians. Similarly, Kogan and Romano (2016a) showed evidence that some derived traits in *Saurichthys* Agassiz, 1834, which Brough (1936) grouped in

https://doi.org/10.1017/jpa.2019.18 Published online by Cambridge University Press

'Subholostei,' were acquired convergently in other taxa (e.g., reduction of squamation). Such hypotheses of convergence ought to be tested in future cladistic analyses.

Series Neopterygii Regan, 1923
Superdivision Holostei Müller, 1845, emend. Grande, 2010
Family Parasemionotidae Stensiö, 1932
Genus *Candelarialepis* new genus

Type species.—*Candelarialepis argentus* n. gen. n. sp., by monotypy.

Diagnosis.—As for the type species by monotypy.

Etymology.—The genus name is composed of two words: (1) Candelaria, the locality of origin, and (2) *to lepos* (το λέπος, ancient Greek), meaning 'scale.'

Remarks.—*Candelarialepis* n. gen. is referred to Parasemionotidae Stensiö, 1932 due to overall similarities with other members of this family. A new genus is erected, for example, due to the presence of a bipartite preopercle and the unique scale ornamentation.

Candelarialepis argentus new species
Figures 8–10

Holotype.—NMMNH P-57423 is preserved as part (NMMNH P-57423a; Figs. 8, 9.1, 10.1) and counterpart (NMMNH P-57423b; Figs. 9.2, 10.2). Silicone casts of P-57423a and P-57423b have been prepared for this study.

Diagnosis.—Large parasemionotid (≥250 mm standard length) with bipartite preopercle, composed of a large dorsal and a large ventral plate (both canal-bearing), with smaller plates in between; anterior scales with dorsal peg and large anterodorsal process (small anterodorsal process in *Albertonia*, *Broughia*), free field ornamentation in anterior scales consisting of ridges that run parallel to the posterior and ventral scale margins and tubercles, posterior scales are smooth (scales either smooth or with longitudinal ridges in other parasemionotids); pectoral fin enlarged (very large in *Albertonia*, *Watsonulus*, *Icarealcyon*, small in other parasemionotids); body deepened (very deep in *Albertonia*, slender in most parasemionotids).

Occurrence.—From the lower Candelaria Formation (middle-upper Dienerian, Lower Triassic) of the eastern Candelaria Hills (Esmeralda County, Nevada, USA).

Description.—The fossil is nearly complete, with only the caudal fin missing, and has a preserved length of ~270 mm. Specimen P-57423a shows the imprints of the bones of the left side of the head, mostly in lateral view, while P-57423b includes the imprints of several of the same bones of the left side of the skull (mostly in medial view) and a few bones from the right side in lateral view (ornamented surfaces). The right side is disarticulated. Identifications of bones are based on comparisons with the parasemionotid *Watsonulus eugnathoides* (Piveteau, 1934) from the Early Triassic of Madagascar (Olsen, 1984; Grande and Bemis, 1998).

Neurocranium.—The neurocranium is exposed in NMMNH P-57423b (Fig. 9.2). Features such as the postorbital process, the anteroventral myodome, or the foramina for the optic and oculomotor nerves may be visible, but are too poorly preserved for a sound description.

Jaws.—The left lower jaw is preserved in situ and is complete (Figs. 9, 10). A poorly preserved fragment of the right lower jaw is possibly preserved in the anterior part of the fossil, interpreted as such due to its ornamentation and indicated presence of a sensory canal. The description is based only on the left lower jaw because it is much better preserved. The lower jaw is relatively short and posteriorly deep, with a pronounced and rounded coronoid process. The lateral side, which is well exposed in P-57423a (Figs. 9.1, 10.1), is composed of the dentary, angular, surangular, and possibly the retroarticular. The dentary is the largest of these bones and forms the anterior part of the lower jaw. It is confined by a long, smoothly sigmoid ventral boundary, being anteriorly concave and posteriorly convex, a long dorsal margin that can be divided into a straight (toothed) anterior part and a sigmoid posterior portion forming part of the coronoid process, and a mostly straight posterior border showing only a small indentation at the base of a small posteroventral process. The posteroventral portion of the mandible is mostly formed by the angular. This bone is bounded by deeply convex posterior and ventral margins and a short, straight dorsal border. Ventral to the angular is a narrow element, the retroarticular, whose boundary with the angular is difficult to trace. The posterodorsal part of the lower jaw is formed by the surangular, which makes a rounded posterodorsal margin. This bone shapes the posterior half of the coronoid process. Just anterior to the coronoid process, a small, toothed portion of the prearticular is visible in lateral view (Figs. 9.1, 10.1). The medial side of the lower jaw is exposed in P-57423b (Figs. 9.2, 10.2), showing the lingual surfaces of the dentary, angular, surangular, and retroarticular. The prearticular, preserved in situ (Figs. 9.2, 10.2), has a somewhat triangular shape, being bounded by a short, nearly straight anterodorsal, a longer, concave posterior, and a mostly straight ventral border. It is not known whether coronoids were developed rostral to the prearticular due to the incomplete preservation of this part.

The lateral ornamentation of the dentary, angular, and surangular consists of tubercles, which are coarse along the ventral margins of the angular and dentary. In the posteroventral part of the dentary, a few thick, anteroposteriorly trending striae are developed, too. The retroarticular appears to be smooth. The lingual side of the prearticular is covered with small teeth, which increase slightly in size near the dorsal margin of this element (well visible on the cast of P-57423b; Fig. 10.2). The dorsal border of the dentary bears numerous close-set, conical teeth. The prearticular teeth are also close-set and conical, like those on the dentary. The dentary and angular are both pierced by the mandibular sensory canal, which closely parallels the ventral margins of these bones. The canal opens in pores laterally, well visible in P-57423a (Fig. 9.1). The external surfaces of the dentary and angular face laterally in the dorsal part of these bones, whereas in the more ventral portions the external surface face ventrally (i.e., the ventral part is curved medially). Rostrally, the lower jaw is curved medially.

https://doi.org/10.1017/jpa.2019.18 Published online by Cambridge University Press

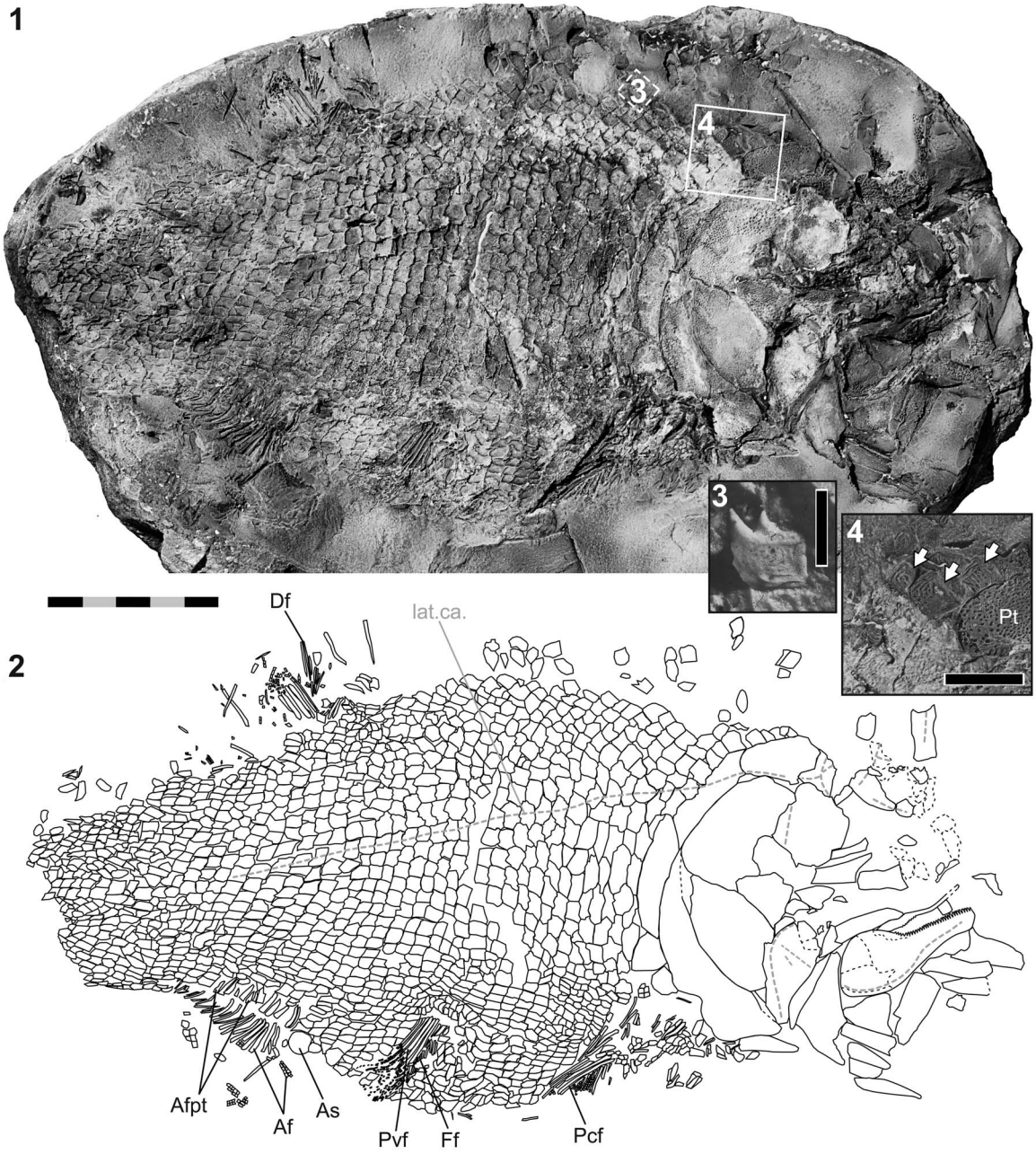

Figure 8. *Candelarialepis argentus* n. gen. n. sp. from the middle-late Dienerian of the Candelaria Hills (Esmeralda County, Nevada, USA). (**1**) Part a of NMMNH P-57423 (enhanced with ammonium chloride); (**2**) interpretive drawing of **8.1**; (**3**) close-up view of a scale (cast of part b of NMMNH P-57423; position indicated in **8.1**); (**4**) close-up view of the scales immediately behind the posttemporal and supracleithrum (position indicated in **8.1**). White arrows in **8.4** point to the scales showing the peculiar ornamentation. Anterior is right in **8.1, 8.2** and **8.4**, and left in **8.3**. Scale bar measures 50 mm (total) in **8.1** and **8.2**, 5 mm in **8.3**, and 10 mm in **8.4**. Abbreviations: **Af**, anal fin (lepidotrichia); **Afpt**, pterygiophores of the anal fin; **As**, pre-anal scale; **Df**, dorsal fin (lepidotrichia); **Ff**, fringing fulcrum; **lat.ca.**, lateral line sensory canal; **Pcf**, pectoral fin (lepidotrichia); **Pt,** posttemporal; **Pvf**, pelvic fin (lepidotrichia).

The upper jaw is very fragmentarily preserved. Presumably, the posterior portion of the left maxilla is seen in situ on both part and counterpart (Figs. 9, 10). The lateral surface of the elongate anterior portion of the right maxilla is probably visible as an imprint on part b (Figs. 9.2, 10.2). This element is curved towards the left side of the animal (i.e., medially), implying that it belonged to the right branch of the upper jaw, thus supporting our interpretation as the right maxilla. The maxilla is short, with a low posterior portion. The lateral surface is covered with fine tubercles. Teeth are not present. Posterodorsally, the right maxilla articulates with an element that is ornamented with horizontal striae. Topologically, this bone may correspond to the supramaxilla (Figs. 9.2, 10.2), although its relatively large size poses doubt on such an interpretation. A slender, elongate bone fragment neighboring the putative left maxilla in P-57423a is tentatively interpreted as the right ectopterygoid (Figs. 9.1, 10.1). This bone cannot belong to the right maxilla because it is situated medially to this element. The anterior portion of the ectopterygoid is bent towards the left side of the skull, hence opposite to the curvature of the adjacent left branch of the lower jaw (thus

https://doi.org/10.1017/jpa.2019.18 Published online by Cambridge University Press

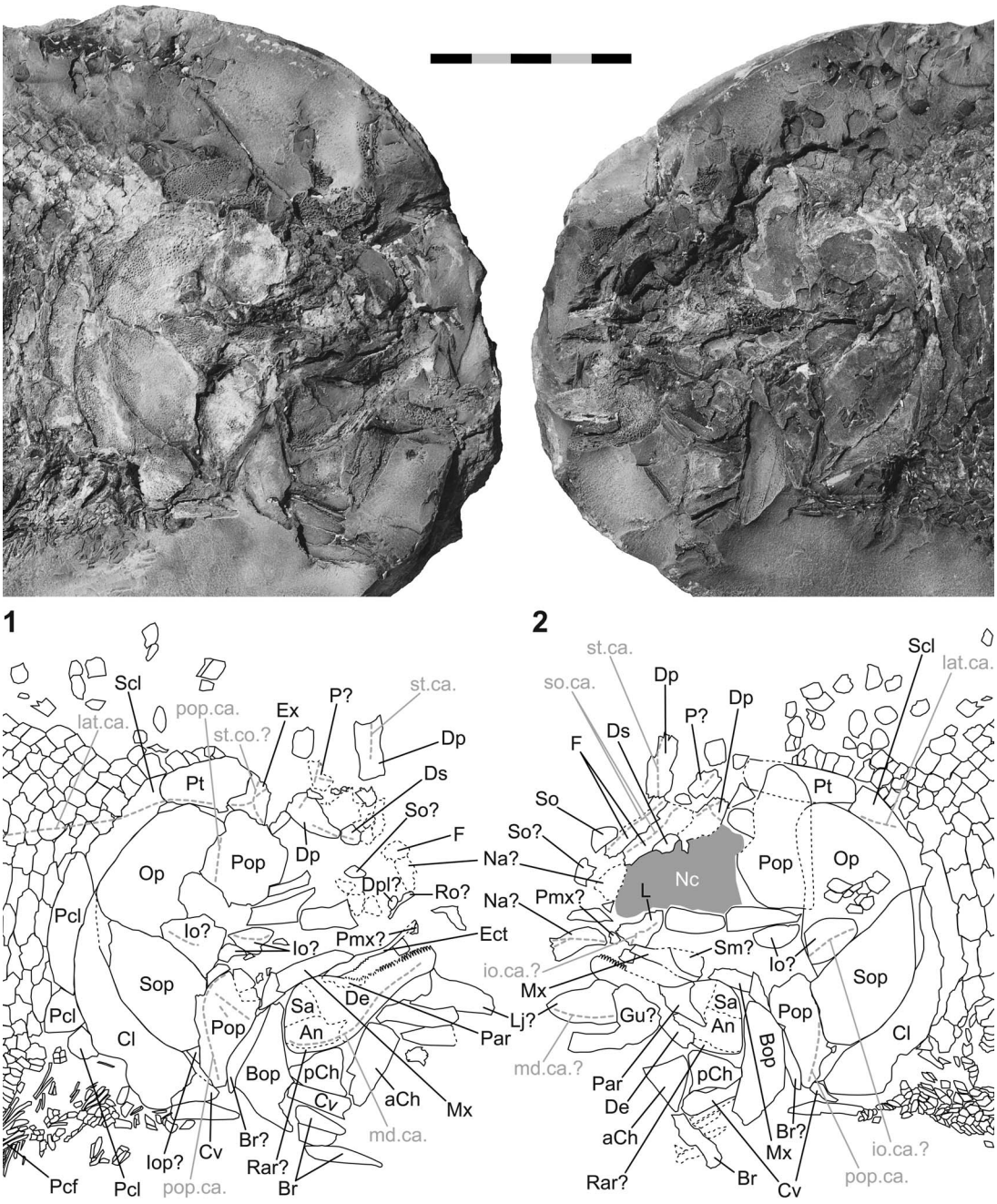

Figure 9. *Candelarialepis argentus* n. gen. n. sp. from the middle-late Dienerian of the Candelaria Hills (Esmeralda County, Nevada, USA). (**1**) Close-up of the anterior body portion of part a of NMMNH P-57423 (enhanced with ammonium chloride) above, with a drawing thereof below; (**2**) close-up of the anterior body portion of part b of NMMNH P-57423 (enhanced with ammonium chloride) above, with a drawing thereof below. Scale bar measures 50 mm (total). Abbreviations: **aCh**, anterior ceratohyal; **An**, angular; **Bop**, branchiopercle; **Br**, branchiostegal ray; **Cl**, cleithrum; **Cv**, clavicle; **De**, dentary; **Dp**, dermopterotic; **Dpl**, dermopalatine; **Ds**, dermosphenotic; **Ect**, ectopterygoid; **Ex**, extrascapular; **F**, frontal; **Gu**, gular plate; **Io**, infraorbital bone; **io.ca.**, infraorbital sensory canal; **Iop**, interopercle; **L**, lachrymal; **lat.ca.**, lateral line sensory canal; **Lj**, lower jaw; **md.ca.**, mandibular sensory canal; **Mx**, maxilla; **Na**, nasal; **Nc**, neurocranium; **Op**, opercle; **P**, parietal; **Par**, prearticular; **Pcf**, pectoral fin (lepidotrichia); **pCh**, posterior ceratohyal; **Pcl**, postcleithrum; **Pmx**, premaxilla; **Pop**, preopercle; **pop.ca.**, preopercular sensory canal; **Pt**, posttemporal; **Rar**, retroarticular; **Ro**, rostral bone; **Sa**, supraangular; **Scl**, supracleithrum; **Sm**, supramaxilla; **So**, supraorbital; **so.ca.**, supraorbital sensory canal; **Sop**, subopercle; **st.ca.**, supratemporal sensory canal; **st.co.**, supratemporal commissure.

supporting our view that the bone in question belongs to the right side of the jaw). Minute teeth are developed along the ventral margin of the ectopterygoid (Fig. 10.1). Two fairly small, tooth-bearing elements found disarticulated in the rostral area of the fossil are tentatively interpreted as the premaxilla and dermopalatine, respectively (Fig. 10.1). The premaxilla is small and equipped with at least three teeth that are slightly larger than the rostral teeth of the dentary. The dermopalatine is larger than the premaxilla. It is plate-like and has a subrectangular shape. A row of close-set teeth is developed on its surface (Fig. 10.1). This bone is identified as the dermopalatine due to overall resemblance with the dermopalatine of *W. eugnathoides* (cf., Olsen, 1984, fig. 13b).

Preopercle and operculogular series.—Several elements posterior and posterodorsal to the jaw bones are identified as

https://doi.org/10.1017/jpa.2019.18 Published online by Cambridge University Press

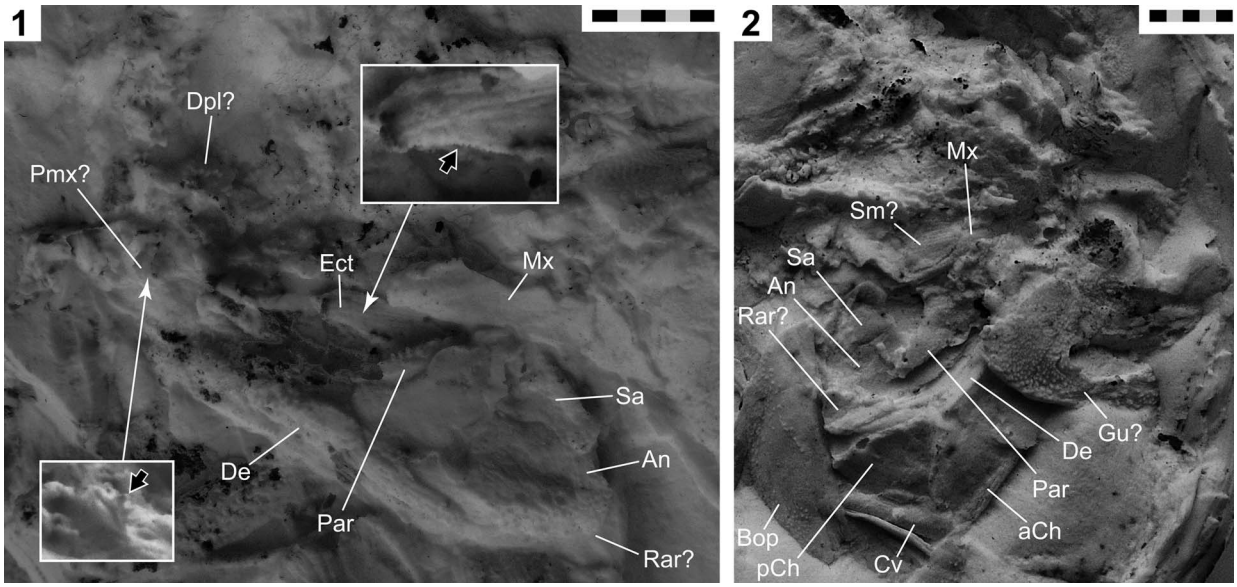

Figure 10. *Candelarialepis argentus* n. gen. n. sp. from the middle-late Dienerian of the Candelaria Hills (Esmeralda County, Nevada, USA). (**1**) Close-up view of the cranial area of the silicone cast of part a of NMMNH P-57423, with jaw bones and selected other elements labeled; (**2**) close-up view of the cranial area of the silicone cast of part b of NMMNH P-57423, with jaw bones and selected other elements labelled. White boxes in **10.1** show magnified views of the putative premaxilla (bottom) and ectopterygoid (top) in different angles than the image in **10.1**. Black arrows point to teeth. Scale bars measures 10 mm (total) in **10.1** and **10.2**. Abbreviations: **aCh**, anterior ceratohyal; **An**, angular; **Bop**, branchiopercle; **Cv**, clavicle; **De**, dentary; **Dpl**, dermopalatine; **Ect**, ectopterygoid; **Gu**, gular plate; **Mx**, maxilla; **Par**, prearticular; **pCh**, posterior ceratohyal; **Pmx**, premaxilla; **Rar**, retroarticular; **Sa**, supraangular; **Sm**, supramaxilla.

parts of the left preopercle (Fig. 9). On the basis of their distribution pattern, we infer that the preopercle consisted mainly of two large, plate-like parts, a dorsal and a ventral one. The ventral portion has a roughly triangular outline, with a long, sigmoid anterior margin (convex dorsally and concave ventrally), a short, convex anterodorsal margin, and a long, convex posterior border. The dorsal extremity of the ventral preopercular plate incorporates at least two smaller elements, which are partially fused to the larger plate (Fig. 9.1). The dorsal preopercular plate is higher than long, and slightly larger than the ventral one (Fig. 9.2). The precise outline of the dorsal plate cannot be deduced due to fragmentary preservation. The preopercular sensory canal is well visible in the ventral plate (Fig. 9.1). The canal runs medially in the narrow, lowermost region, and close to the posterior bone margin in the dorsal region. A segment of this sensory canal can be traced in the dorsal preopercular plate, running close to the caudal bone margin. Two pit lines are faintly visible on the ventral preopercular plate: a dorsal one, corresponding to the horizontal pit line, and a shorter ventral one, interpreted as the vertical pit line (Fig. 9.1). The ornamentation of the preopercular plates consists of tubercles. Some slightly enlarged tubercles are observed in the lowermost area of the ventral bone, especially in vicinity of the sensory canal.

The left opercle, subopercle, and possibly the interopercle are still in situ, whereas the gular plate, branchiostegal rays, and branchiopercle are found dislocated ventral to the cranium (Fig. 9). The opercle, the largest element of the operculogular series, is confined by a long, convex posterodorsal margin, and a straight ventral border. The subopercle, slightly smaller than the opercle, has a long, convex posteroventral border and a straight dorsal margin. The anterior borders of the opercle and subopercle are covered by other cranial bones. The ornamentation of the opercle and subopercle is mostly composed of tubercles, of similar size and with a comparable density as those on the preopercle. The tubercles increase in size in the anterodorsal part of the opercle. A small portion of the left interopercle may be seen anteroventral to the subopercle (Fig. 9.1); the remaining part of this element is covered by the ventral preopercular plate. At least three branchiostegal rays are preserved. Each one has an elongate, subrectangular outline. A single, large element preserved anterior to the left ventral preopercular plate is interpreted as a possible branchiopercle (Figs. 9, 10.2). It is much larger than the branchiostegal rays, with a distinctly convex lateral surface. A large, plate-like fragment anterior to the lower jaw may correspond to the median gular. It probably had an ovoid shape, being somewhat longer than wide. The ornamentation of the branchiostegals and branchiopercle consists of tubercles, which are less densely spaced than on the opercle and subopercle. The gular is densely covered with tubercles. Coarse tubercles and short striae occur near the lateral bone margins.

Hyoid arch.—At least the anterior and posterior ceratohyals are preserved, located ventral to the lower jaw (Figs. 9, 10.2). Both ceratohyals are plate-like. The anterior one is imperfect, but seemingly had an elongate shape. It is marked by a conspicuous, reticulated surface structure along its ventral margin (like in *W. eugnathoides*; cf., Grande and Bemis, 1998, fig. 416). The posterior ceratohyal has a triangular outline.

Dermal skull roof.—The dermal skull roof is very fragmentarily preserved (Fig. 9). A small, bow-shaped bone, being overlapped by one of the premaxillae, could correspond to the rostral, but it is inadequately preserved. An isolated element preserved in the rostral area (Fig. 9.2) contains a seemingly triradiate sensory canal. It possibly pertains to the right nasal (cf., Grande and Bemis, 1998, fig. 415). The left nasal is possibly preserved in

https://doi.org/10.1017/jpa.2019.18 Published online by Cambridge University Press

situ, but too incomplete for sound description. Posterior to the left nasal bone are the large, paired frontals. These elements are elongate and consist of a mediolaterally broad postorbital portion, and a slightly narrower anterior segment. Rostrally, the frontals extend to about the level of the center of the orbit. Each frontal is bounded by a long, serrated medial margin, and a straight posterior border. Its anterior confinement is not well visible, but was probably straight. The lateral border of the frontal is, as far as can be seen, anteriorly and posteriorly straight, and sigmoid in its middle portion. A sensory canal carrying bone fragment posterior to the left frontal may pertain to the corresponding parietal. Probably both dermopterotics are preserved in the posterolateral part of the dermal skull roof. The dermopterotic is longer than wide and bears two sensory canals that run perpendicular to one another. One of these canals, belonging to the supratemporal section of the lateral line, is anteroposteriorly oriented and passes over into the dermosphenotic rostrally. In the posterior part of the dermopterotic, a second canal runs in mediolateral direction, seemingly continuing medially through the parietal. Sections of the supraorbital sensory canal are visible within the frontals and the nasal. The ornamentation of the dermal cranial roof, where visible, consists of fairly coarse tubercles, generally larger than those on the bones of the operculogular series. In the posterior part of the skull roof, the tubercles become oblong and occasionally very large.

Circumorbitals.—Small, plate-like bones preserved lateral to the dermal cranial roof are interpreted as the dermosphenotic and supraorbitals. A keystone-shaped element that is firmly connected to the left frontal is identified as the dermosphenotic (Fig. 9.2). Two serially arranged bones on the right side of the dermal skull roof, which are slightly larger than the dermosphenotic, correspond to supraorbitals. Another supraorbital, probably from the left side of the head, is dislocated from its original position (Fig. 9.1). The supraorbitals are covered with dense, relatively coarse tubercles similar to those on the dermal skull roof.

Regarding the bones of the infraorbital series, only the right lachrymal is preserved in situ (Fig. 9.2). This bone has a subtriangular shape, being higher than long, and contains a section of a sensory canal. The external surface is covered with fine tubercles. Three elements, now located between the dorsal and ventral preopercular plates, either belong to the infraorbital or suborbital series (Fig. 9). The most posterior of these bones, which is the largest one, was possibly located posteroventrally to the eye in vivo (jugal). Impressions of a sensory canal may be visible on the medial surface of this bone (Fig. 9.2). The two smaller infraorbital bones, now placed just anterior to the former, may have originally framed the ventral or posterior confinements of the orbital opening. The three infraorbital bones share the same conspicuous ornamentation, consisting of coarse tubercles and reticulate ridges. The tubercles on the lateral surface of the three dislocated infraorbital bones are larger than those on the preopercular plates, rendering an allocation of these three elements to the preopercle unlikely.

Shoulder girdle.—The pectoral girdle is composed of four dermal bones: posttemporal, supracleithrum, cleithrum, and clavicle. The elements of the left half of the shoulder girdle are in situ, whereas of those of the right side, only the clavicle is preserved and dislocated (Fig. 9). The posttemporal consists of an external plate and a rod-like ventral process, issuing from the medial surface of the plate-like portion, near its lateral margin. The ventral process itself is covered by the adjacent bones, but its base is visible in P-57423a. The plate-like part is longer than wide and has an ovoid outline. Its external surface is covered with tubercles, except for the very anterior region. A sensory canal traverses the bone along its lateral border. Posteroventrally, the posttemporal is still connected to the supracleithrum, laterally covering a small area of the latter. The supracleithrum is a slender, plate-like bone with a trapezoidal shape. It is bounded by long, parallel posterodorsal and anteroventral margins and short, straight posterior and dorsal borders. The external surface of the supracleithrum is covered with tubercles of comparable size to those on the opercle and subopercle. Within its upper portion, the supracleithrum is pierced by a section of the lateral line sensory canal, traversing the bone obliquely in anteroposterior direction (Fig. 9.2).

The large cleithrum, placed ventral to the supracleithrum, has a broadly triangular outline (crescent-shaped). It is confined by a long, concave anterodorsal margin, a short, straight ventral border, and a long, sigmoid posterior margin, being dorsally convex and ventrally concave. The external surface is distinctly bent: the area along its anterodorsal border faces anterolaterally, whereas the posterodorsal and posteroventral regions of the cleithrum face laterally. Most of the lateral surface is ornamented with distinct, dorsoventrally running, interrupted ridges, which show anastomozation. Coarse, rounded tubercles occur in the ventral area. A strong ridge marks the anteroventral part of the medial surface of the cleithrum (preserved as an impression on the left cleithrum of P-57423b; Fig. 9.2). The endochondral shoulder girdle is not visible. The left clavicle is observed still in articulation with the corresponding cleithrum, while the right clavicle is located anteroventral to the branchiopercle. The clavicle is much smaller than the cleithrum and has a rectangular, elongate shape. Its external surface is ornamented with distinct, close-set, anastomozing striae that run perpendicular to the longitudinal axis of the bone, and tubercles locally (similar to *W. eugnathoides*; Grande and Bemis, 1998, fig. 416).

The supracleithrum and cleithrum are bordered by a large, deep postcleithrum. Two additional, smaller postcleithra are seen ventral to this element (Fig. 9). The postcleithra are covered with tubercles and vertical ridges, similar to those on the cleithrum. Wedged between the posttemporal and dermal skull roof is another, probably paired element: the extrascapular. The left extrascapular is preserved in situ (Fig. 9.1). This plate-like bone is anteroposteriorly short and of rectangular shape. Posteriorly, it partly overlaps an unornamented area on the left posttemporal. The extrascapular is covered with tubercles, and is traversed by four pore canals that meet in the center of the bone. The posterolateral and anterolateral canals correspond to the lateral line (or otic canal, respectively), whereas the two medially directed branches may belong to the supratemporal commissure, and perhaps to a link with the supraorbital sensory canal, respectively.

Paired and unpaired fins.—The pectoral, pelvic, dorsal, and anal fins are preserved in situ, but are not complete (Fig. 8.1, 8.2). The relatively large pectoral fin inserts at the level of the concave lower part of the cleithrum's posterior margin. The

https://doi.org/10.1017/jpa.2019.18 Published online by Cambridge University Press

radials are not exposed. The lepidotrichia of the pectoral fin are long and segmented, with long proximal and short, box-shaped distal units. The fin rays are distally branched. The ventral (pelvic) fin is placed midway between the pectoral and anal fins. It is short-based and consists of approximately seven fin rays. Each lepidotrichium is long and segmented, with long units at the base and much shorter ones distally. The fin rays are distally bifurcated. A few fringing fulcra are seen along the leading edge of the ventral fin. The anal fin is long-based, comprising ~20 lepidotrichia. The basal lepidotrichial segments of the anal fin are preserved in situ, being relatively long. Several short, box-shaped distal lepidotrichial segments are found scattered nearby. Some lateral scales at the base of the anal fin are missing, exposing a single row of pterygiophores. The exact number of these elements cannot be determined, but they relate as 1:1 to the fin rays. The dorsal fin is located slightly in front of the anal fin, but begins a few scale rows caudal to it (Fig. 8.1, 8.2). Although only a few fin rays are preserved in situ, the dorsal fin was probably long-based, judging from the distribution of in situ preserved basal lepidotrichial segments. The dorsal fin is composed of long fin ray segments at the base and much shorter units distally. The lepidotrichia ramify distally.

Squamation.—The body of P-57423 is fusiform and relatively deep, with the maximum dorsoventral depth being found at a level slightly in front of the pelvic fins (Fig. 8). The squamation is composed mostly of rhombic scales, arranged in S-curved, subvertical rows. The course of the lateral line sensory canal can be traced along some scales situated between the shoulder girdle and the anal and dorsal fins. About 45 scale rows are counted along the inferred path of the lateral line (between the supracleithrum and the caudal end of the fossil). The scales on the flanks are slightly larger than those in the dorsal and ventral parts, and the depth of the scales decreases successively towards caudally.

The rhombic scales exhibit a large free field posteroventrally, and narrow, smooth anterior and dorsal areas that are laterally covered by the neighboring scales. The free field of the anterodorsal scales (Fig. 8.3, 8.4) is ornamented with ridges that are mostly oriented parallel to the posterior and ventral margins of the scale. The ridges may be interrupted, especially in the anterodorsal part of the free field. The scales immediately posterior to the postcleithra are ornamented with dorsoventrally directed ridges, similar to those on the postcleithra. In other parts of the body, the free field of the scales is smooth. Most scales do not show a denticulate hind margin, though a few scales on the cast of part b exhibit very weak serrations. A dorsal spine for peg-and-socket articulation and a slightly larger anterodorsal process are developed on scales in the anterodorsal and anteroventral part of the trunk (Fig. 8.3). Both features are seemingly absent on scales posterior to the level of the pelvic fins. At least one specialized scale is found anterior to the anal fin (Fig. 8.1, 8.2). This pre-anal scale has a circular shape and is enlarged compared to the neighboring scales. It is ornamented with concentric ridges.

Etymology.—The name *argentus* (Latin) means 'silver,' in reference to the historic silver mining activity in the Candelaria area and other locales in Nevada (Knopf, 1922; Page, 1959).

Materials.—BSPG 1984 I 238 (*Albertonia cupidinia* [Lambe, 1916]), MNHN.F.MAE 11, MAE 33, MAE 34, MAE 42, MAE 108, MAE 583 (*Watsonulus eugnathoides* [Piveteau, 1934]), PIMUZ A/I 4360 (cf. *Watsonulus* cf. *eugnathoides*; Romano et al., 2016b), PIMUZ T 1109, T 3090, T 3140, T 4315 (*Aetheodontus besanensis* Brough, 1939; Bürgin, 1992).

Remarks.—The overall morphology of NMMNH P-57423 is reminiscent of *Watsonulus eugnathoides* (Piveteau, 1934) and other Parasemionotidae Stensiö, 1932 (= Ospiidae Stensiö, 1932), rendering a close affinity to this family probable. Parasemionotidae were a globally distributed family, represented by at least 18 species in the Early Triassic (see Romano et al., 2016b for a recent summary). There are also younger, Triassic occurrences that have been referred to this family (Wade, 1935, 1940; Griffith, 1977; Beltan, 1984a). However, due to inadequate preservation and differences in morphology, for instance the narrow dorsal portion of the preopercle of some of these taxa (e.g., Tintori, 1990), their close relationship with Parasemionotidae seems questionable (also see Grande and Bemis, 1998; Arratia and Herzog, 2007; Li, 2009). Similarities between P-57423 and parasemionotids include the broad preopercle, subdivided into smaller plates, and the general morphology of the lower jaw (e.g., Lehman, 1952; Olsen, 1984; Grande and Bemis, 1998; Liu et al., 2002; Tong et al., 2006; Li, 2009). The general shape, orientation, and size of the area occupied by the preopercle of P-57423 are most similar to parasemionotids and some 'subholosteans' compared to other actinopterygians (see summary of preopercular morphology among actinopterygians in Mickle, 2013). However, P-57423 clearly differs from 'subholosteans' because its preopercle is evidently not connected to the maxilla, and there is a well-developed coronoid process, formed by the dentary and surangular.

The pattern of fragmentation of the dorsal portion of the preopercle has been used to distinguish species of Parasemionotidae, though some intraspecific variation was recognized (Piveteau, 1934; Lehman, 1952; Lehman et al., 1959; Grande and Bemis, 1998). In most parasemionotids, the preopercle consists of a large ventral plate and a varying number of smaller, dorsal ossifications (suborbitals; e.g., Lehman, 1952; Lehman et al., 1959; Grande and Bemis, 1998). A division into large, canal-bearing, dorsal and ventral plates, and smaller, anamestic plates in between, is known solely from P-57423; nevertheless, a somewhat similar pattern is indicated in Wade's (1940) reconstruction of the ?parasemionotid *Promecosomina* Wade, 1935 from Middle Triassic freshwater deposits of New South Wales (Australia).

In P-57423, the scales show a peculiar ornamentation in the anterodorsal trunk region (ridges running parallel to the posterior and ventral margin of the scale), whereas in the remaining part of the body, the free field is smooth. In parasemionotids, where known, the scales are either smooth (Priem, 1924; Liu et al., 2002; Tong et al., 2006) or ornamented with anteroposteriorly running ridges (Lambe, 1916; Stensiö, 1932; Piveteau, 1934; Lehman, 1952). Longitudinal ridges also characterize the scales of the neopterygian *Panxianichthys* Xu and Shen, 2015, whereas the free field is smooth in *Peia* Li, 2009. Weak, concentric ridges have been described in the Middle Triassic perleidiform *Aetheodontus* Brough, 1939 (Bürgin, 1992), but

https://doi.org/10.1017/jpa.2019.18 Published online by Cambridge University Press

the pattern is different in P-57423 (personal observation, CR). Ornamented scales (tubercles) in the anterodorsal body portion (and otherwise smooth scales) were described in the semionotiform *Lophionotus* Gibson, 2013 from Late Triassic freshwater deposits of Utah (USA). In many parasemionotids as well as other actinopterygians with rhombic scales, the hind margin of the scales is denticulated (e.g., Stensiö, 1932; Brough, 1939; Lehman, 1952; Gibson, 2013; Sun et al., 2017), while in P-57423 denticles are mostly absent. Stensiö (1932) presented evidence for ontogenetic loss of scale denticulation in the parasemionotid *Broughia* Stensiö, 1932 (Early Triassic, Greenland), indicating that this character has limited taxonomic use. The anterior scales of P-57423 bear large anterodorsal processes, while such processes are small in *Albertonia* Gardiner, 1966 and *Broughia* (Lambe, 1916; Stensiö, 1932).

The supramaxilla of P-57423, if identified correctly, has a large dorsoventral expansion. Although this element is imperfectly preserved, its ornamentation composed of rostrocaudally directed striae is typical for the supramaxilla of early neopterygians (e.g., Boni, 1937; Arratia and Herzog, 2007). Relatively large supramaxillae are developed in some neopterygians (e.g., Wade, 1935, 1940; Boni, 1937; Arratia and Herzog, 2007; Sun et al., 2017), but this bone is normally small (López-Arbarello et al., 2016). Parasemionotids exhibit slender supramaxillae that are usually ornamented with tubercles (Stensiö, 1932; Lehman, 1952; Lehman et al., 1959; Grande and Bemis, 1998; Li, 2009). Striae are, nonetheless, visible in the anterior part of the supramaxilla of some specimens of *Watsonulus* Brough, 1939 (e.g., MNHN.F.MAE 11; Piveteau, 1934, pl. 9, figs. 1, 1a; MNHN.F.MAE 2507, Grande and Bemis, 1998, fig. 415). Better-preserved material is needed to test whether the large size of the supposed supramaxilla of NMMNH P-57423 is a diagnostic feature or not. With a standard length of ~270 mm, P-57423 is one of the largest parasemionotids. Its size is only matched by *Albertonia* from Canada (Lambe, 1916; BSPG 1984 I 238) and *Icarealcyon* Beltan, 1980a from Madagascar (Beltan, 1984b). Most parasemionotids are small, with standard lengths of ~100–200 mm (Stensiö, 1932; Lehman, 1952; Schaeffer and Mangus, 1976; Tong et al., 2006). Although the pectoral fin of NMMNH P-57423 is incomplete, it appears to be enlarged. This fin is fairly large in *Albertonia*, *Watsonulus*, and *Icarealcyon*, but small in other parasemionotids.

In light of the current evidence, specimen P-57423 is referred to a new genus and species, *Candelarialepis argentus* n. gen. n. sp., which is provisionally referred to Parasemionotidae due to overall resemblances to other members of this group, pending a thorough systematic revision of this family, which is beyond the scope of this publication.

Actinopterygii indet.
Figure 11

Occurrence.—From the lower Candelaria Formation (middle-upper Dienerian, Lower Triassic) of the eastern Candelaria Hills (Esmeralda County, Nevada, USA).

Description.—Four unequivocal actinopterygian remains (PIMUZ A/I 4727, A/I 4728, A/I 4731, A/I 4732), which lack diagnostic features for identification at low taxonomic rank. Specimen A/I 4728 was recovered in situ within the shale, while the three others were found as float. The fossils represent more than one taxon.

PIMUZ A/I 4728.—This is an incomplete, largely articulated, mid-sized actinopterygian (estimated standard length ~250–300 mm). Part a of specimen A/I 4728 (Fig. 11.1) contains the body (squamation) and some bones of the skull and shoulder girdle, as well as parts of the dorsal and anal fins. Portions of the squamation, fin rays, and several dermal bones are also preserved on a few noncontiguous fragments of the counterpart of the same nodule.

Of the dermal bones of A/I 4728, only the left cleithrum can be confidently identified. It is preserved anterior to the dorsal fin (Fig. 11.1). The cleithrum is bounded by a short, straight anterior margin, a long, convex posteroventral border marked by an indentation at the level of insertion of the pectoral fin, and a long, equably concave anterior confinement. The dorsal extremity of the cleithrum is incomplete. The convex external surface is ornamented with coarse, anastomosing striae, radiating from the center of the cleithrum, which is situated just anterior to the aforementioned indentation. Some striae running parallel to the anterior margin are observed in the anterior part of this element. The other, plate-like bones of A/I 4728 are ornamented with either coarse tubercles or thick, bifurcating striae.

The squamation consists of subvertical rows of large, rhombic scales. Approximately 35 rows are developed along the flanks between the anterior and posterior ends of the fossil. The scales along the flanks in the anterior body portion are about as deep as long, whereas those in the caudal, dorsal, and ventral body regions are much longer than deep. The ornamentation of the free field is preserved predominantly on the scales in the anterodorsal trunk portion. It consists of a few, anteroposteriorly running, gently meandering ridges, which become more distinct near the ventral scale margin.

The dorsal and anal fins of A/I 4728 are both situated in the caudal region of the body and are opposed to each other. The dorsal fin consists of fine lepidotrichia, each composed of a long proximal portion and shorter, elongate distal segments. Bifurcation is observed on some fin rays. It is not possible to count the number of fin rays because they are mostly disarticulated, but they appear to be numerous. The anal fin rays are mostly not visible. About 14 pterygiophores are preserved in situ at the base of this fin, but the posterior part of the fin base is missing. There are a few thin fin ray segments dispersed nearby. Because the dorsal and anal fins are often built similarly in coeval actinopterygians, we infer that the number of lepidotrichia may have exceeded that of the pterygiophores in A/I 4728.

PIMUZ A/I 4727.—This specimen is preserved on two halves of a nodule, as part a and part b, respectively, showing the disarticulated remains (dermal bones, scales, fin rays) of a mid-sized actinopterygian (Fig. 11.2). The plate-like dermal bones show rather coarse surface ornamentation. Some of these elements are covered with thick, anastomosing striae, while others exhibit predominantly tubercles. Due to the fragmentary preservation, the dermal bones cannot be identified. The scales of A/I 4727 have a rhombic outline (Fig. 11.3). Some of them are about as deep as long, while others are distinctly longer than high. Many scales show a dorsal peg and a

https://doi.org/10.1017/jpa.2019.18 Published online by Cambridge University Press

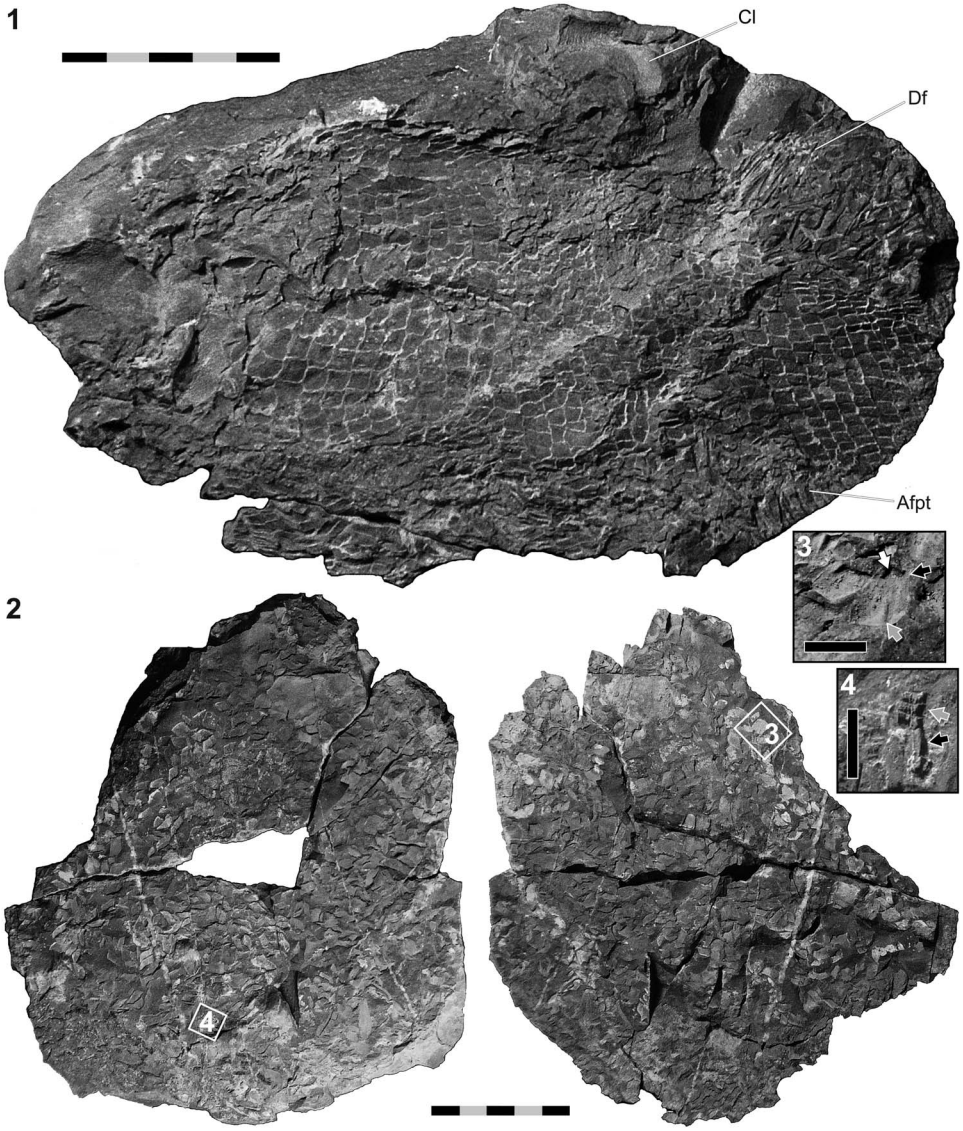

Figure 11. Examples of Actinopterygii indet. from the middle-late Dienerian of the Candelaria Hills (Esmeralda County, Nevada, USA). (**1**) PIMUZ A/I 4728 (part a); (**2**) PIMUZ A/I 4727, part a (left) and part b (right); (**3**) close-up view of the squamation of PIMUZ A/I 4727 (position indicated in **11.2**), showing the dorsal peg (white arrow), the socket on the medial scale surface (gray arrow), and the anterodorsal process (black arrow); (**4**) close-up view of two articulated lepidotrichia of PIMUZ A/I 4727 (position indicated in **11.2**) displaying the segmentation pattern characterized by a long basal segment (black arrow) and several, box-shaped distal segments (gray arrow). Anterior is left in **11.1**. Scale bar measures 50 mm (total) in **11.1** and **11.2**, 10 mm in **11.3**, and 5 mm in **11.4**. Abbreviations: **Afpt**, pterygiophores of the anal fin; **Cl**, cleithrum; **Df**, dorsal fin (lepidotrichia).

ventral socket on their medial surface. Such a peg-and-socket-articulation is not only developed on the deep scales, probably originating from the anterior flank region, but also on some of the elongate scales, supposedly from the posterior, dorsal, or ventral trunk areas. On many scales, a pronounced anterodorsal process is developed. The hind margin of the scales is usually straight, but at least one scale shows serrations. The free field is smooth. Some lepidotrichia are preserved, consisting of either long segments or shorter, box-shaped segments, frequently still in articulation (Fig. 11.4).

PIMUZ A/I 4731 and PIMUZ A/I 4732.—Both specimens require excessive preparation before sound description, but they can be confidently identified as mid-sized actinopterygians based on the exposed skeletal elements. Specimen A/I 4731 shows articulated rhombic scales of comparable size, as in A/I 4728. The scales are subquadrangular. On at least one scale of A/I 4731, there is a small dorsal peg and a similar-sized anterodorsal process. Specimen A/I 4732, on the other hand, shows a dermal bone covered with distinct striae and tubercles. This specimen also preserves the squamation, but it is still enclosed in the matrix.

Remarks.—Based on the visible anatomical features, PIMUZ A/I 4727, A/I 4728, A/I 4731, and A/I 4732 can be referred to Actinopterygii. They clearly belong to more than one species, suggesting that additional taxa are to be found in the Candelaria Formation. Specimens A/I 4731 and A/I 4732 are both too incompletely known and are thus not further discussed here.

Specimen A/I 4728 exhibits a generalized, 'palaeoniscoid' bauplan, characterized by the shape and ornamentation of the

https://doi.org/10.1017/jpa.2019.18 Published online by Cambridge University Press

dermal bones and scales, as well as the relative positions of the dorsal and anal fins, their segmentation pattern, and lepidotrichia to pterygiophore ratio. This morphology is typical for many contemporaneous taxa. There are superficial similarities between PIMUZ A/I 4728 and A/I 4402 (*Pteronisculus nevadanus* n. sp.). However, an attribution of A/I 4728 to *P. nevadanus* n. sp. is not permitted due to the larger size of the scales (relative to body size) and the weaker ornamentation of the scales in A/I 4728. *Pteronisculus* White, 1933 typically has small scales (e.g., Nielsen, 1942; Lehman, 1952; Xu et al., 2014). The incomplete preservation and lack of diagnostic features complicate comparisons of A/I 4728 with other taxa, and it is thus left in open nomenclature.

A peculiar feature of A/I 4727 is the segmentation pattern of the lepidotrichia, consisting of long (basal) segments and numerous, very short (distal) segments (Fig. 11.4). Although a fin ray segmentation pattern composed of long basal segments and distinctly shorter distal units is common among Triassic actinopterygians, long basal segments and box-shaped (i.e., about as high as wide), distally adjoining segments are typical for the dorsal and anal fins of *Candelarialepis argentus* n. gen. n. sp. (Fig. 8.1), other parasemionotids, and some other early neopterygians (cf., Stensiö, 1921, 1932; Lehman, 1952; Bürgin, 1992; Liu et al., 2002; Xu and Shen, 2015; Romano et al., 2016b; Marramà et al., 2017). The phylogenetic meaning of this segmentation pattern needs further exploration. The general morphology of the scales of PIMUZ A/I 4727 and the ornamentation pattern of some dermal bones are also comparable to NMMNH P-57423 (*C. argentus* n. gen. n. sp.). However, referral of PIMUZ A/I 4727 to *C. argentus* n. gen. n. sp. is hindered due to lack of evidence of the typical scale ornamentation of the anterodorsal scales of this species (Fig. 8.3, 8.4); it is thus kept in open nomenclature.

Diversity and body size of Early Triassic bony fishes: state of the art and perspectives

Latitudinal diversity gradient.—Above, we describe the first actinopterygians from the lower Candelaria Formation (Candelaria Hills, Esmeralda County, Nevada, USA), deposited during the middle to late Dienerian (late Induan; Ware et al., 2015), ca. 500 ka after the PTBME (Galfetti et al., 2007; Baresel et al., 2017). Invertebrates (ammonoids, bivalves, ostracodes, serpulids) and conodonts from this formation have been known for decades (e.g., Muller and Ferguson, 1939; Poole and Wardlaw, 1978), but the occurrence of ichthyoliths (fish teeth) has only been casually mentioned (Poole and Wardlaw, 1978), and the presence of articulated fishes was unknown until recently (Brinkmann et al., 2010). The material includes a new species of *Pteronisculus* White, 1933, *P. nevadanus* n. sp. (Turseoidae? Bock, 1959), and two new species referred to new genera, *Ardoreosomus occidentalis* n. gen. n. sp. (Ptycholepidae Brough, 1939) and the holostean *Candelarialepis argentus* n. gen. n. sp. (Parasemionotidae Stensiö, 1932), as well as Actinopterygii indet. belonging to other taxa. The described specimens constitute only part of the collected material and we expect additional taxa to occur in this assemblage. Remarkably, the majority of the collected specimens (~60%) are coelacanths, contrasting with ichthyofaunal compositions of other Early Triassic sites (cf., Nielsen, 1961). Marine osteichthyan macrofossils coeval to those from the Candelaria Hills occur in Madagascar (Kogan and Romano, 2016a) and Spiti (Himachal Pradesh, India; Romano et al., 2016b). Some fishes from Canada are derived from Dienerian strata (Schaeffer and Mangus, 1976; Davies et al., 1997; Wignall and Newton, 2003; Mutter and Neuman, 2009), but most of the Canadian material is of Smithian age (Orchard and Zonneveld, 2009).

There are a couple of other, mostly younger (Smithian/Spathian), marine occurrences of osteichthyan and chondrichthyan fishes in the western United States, such as in central and northeast Nevada (e.g., Koot, 2013; Romano et al., 2017), southeast Idaho (e.g., Goddard, 1907; Romano et al., 2012, 2017, in press), Utah, and California (Koot, 2013). In contrast to most of these sites, fish fossils occur relatively abundantly in the Candelaria Hills. The localities in the present-day western USA were situated on the eastern rim of the Panthalassa Ocean during the Early Triassic, not far from the paleoequator. To our knowledge, the Candelaria Hills represent one of the southernmost occurrences of Triassic fishes from the eastern Panthalassa (López-Arbarello, 2004; Brinkmann et al., 2010; Koot, 2013).

Until the publication of the monumental works on the marine Early Triassic fishes from Spitsbergen, East Greenland and Madagascar (e.g., Stensiö, 1921, 1932; Nielsen, 1942, 1949; Lehman, 1952), almost nothing was known about the fishes from this epoch. These fossil-rich sites were located in mid-latitudes during the Early Triassic. Taking the fossil record at face value, Romano et al. (2016a) highlighted the astonishingly high mid-latitudinal diversity of bony fishes during the Early Triassic, which contrasts with their very low diversity in the equatorial domain. In light of the recently discovered occurrences in the western USA, and those from China (e.g., Liu et al., 2002; Tong et al., 2006; Li, 2009), we infer that the diversity of low-latitudinal Early Triassic fishes is probably still underestimated; therefore, sampling or taphonomic imbalances cannot be ignored as factors contributing to the atypical latitudinal diversity gradient of Osteichthyes after the PTBME (also see Romano et al., 2017 for discussion). We stress, however, that during the Permian-Triassic interval, mid-latitudinal osteichthyan diversity peaked during the Early Triassic (Romano et al., 2016a).

Cosmopolitanism.—The fishes from the Candelaria Hills, as well as those from other Early Triassic (pre-Spathian) localities in the western USA, belong to groups that are known from several coeval sites around the world ('Triassic Early Fish Fauna' of Tintori et al., 2014), underlining the previously recognized cosmopolitan distribution (low β-/γ-diversity) of higher taxa in the wake of the PTBME (Stensiö, 1932; Piveteau, 1935; Schaeffer and Mangus, 1976; Romano et al., 2016a). However, a few, otherwise widespread post-extinction taxa are absent in the collected material, such as the ambush predator *Saurichthys* Agassiz, 1834 or the deep-bodied *Bobasatrania* White, 1932, either of which would be easily identifiable due to their derived morphologies, although their absence could be due to small sample size. These taxa have

https://doi.org/10.1017/jpa.2019.18 Published online by Cambridge University Press

also not yet been described from the Griesbachian–Smithian of China (e.g., Tong et al., 2006; Tintori et al., 2014).

As highlighted by the diagnoses above, the Candelaria Hills actinopterygians are morphologically distinct from their close relatives from Panthalassan sites in higher latitudes (e.g., Stensiö, 1921, 1932; Nielsen, 1942; Schaeffer and Mangus, 1976; Neuman, 2015) and the Tethys Ocean (e.g., Lehman, 1952; Liu et al., 2002; Tong et al., 2006; Li, 2009; Romano et al., 2016b). These differences suggest some early differentiation at the regional level <1.5 Ma after the mass extinction event (Ovtcharova et al., 2006; Baresel et al., 2017). An early differentiation is also exemplified by the intensively studied *Saurichthys* (e.g., Mutter et al., 2008; Kogan and Romano, 2016b). Following the 'Spathian gap' (Romano et al., 2017), the fossil record reveals a distinct peak in global diversity and disparity of bony fishes in the Middle Triassic (Tintori et al., 2014; Smithwick and Stubbs, 2018).

Why are pre-Spathian bony fish assemlages more homogenous globally than Middle Triassic ones? Although the preservation of fishes in Middle Triassic sites, for instance the Luoping Biota (South China) or Monte San Giorgio area (Switzerland/Italy), is better than that in Early Triassic localities, we consider it unlikely that the similarities of pre-Spathian fish assemblages are purely a preservational artefact. Romano et al. (2016b) argued that cosmopolitanism may have been the result of the severity of the PTBME, poorly differentiated Early Triassic habitats (contra Schaeffer and Mangus, 1976), or facilitated circumpangean dispersal due to episodic occurrent low-latitudinal temperature gradients (cf., Brayard et al., 2006). However, these different hypotheses require testing with quantitative data. The pattern of Triassic osteichthyan radiation seems to agree with theoretical modeling of diversifications that are driven by diversity dependent competition (Hautmann, 2014), in which increases in β-diversity initially stagnate (as α-diversity rises) due to low competition between species. An increase in α-diversity is expected in a later stage as a result of niche differentiation, leading to rising β- and γ-diversity.

Body size.—Maximum standard lengths (median and distribution) of osteichthyan species were skewed towards larger sizes during the Lopingian (late Permian) and Early Triassic, and body size was not an extinction factor during the PTBME (Romano et al., 2016a; Puttick et al., 2017). On the contrary, body length distribution of Osteichthyes was skewed towards small sizes in the Middle Triassic ('Triassic Middle Fish Fauna;' Tintori et al., 2014), with many taxa achieving lengths of not more than a few centimeters (e.g., *Aetheodontus* Brough, 1939; *Habroichthys* Brough, 1939; *Prohalecites* Deecke, 1889; *Prosantichthys* Arratia and Herzog, 2007). The vast absence of very small fishes (≤10 cm adult body length) in the Early Triassic and the abundance of such taxa in the Middle Triassic had been anticipated by some authors (e.g., Deecke, 1927; Tintori et al., 2014) and was recently proven using quantitative data (Scheyer et al., 2014; Romano et al., 2016a; Puttick et al., 2017). Although small fishes are most abundant today in low latitudes, Romano et al. (2016a) argued that the significant decrease in body size from the Early to the Middle Triassic is unlikely due to limited data from low-latitudinal, Early Triassic sites because the size decrease is evident across latitudes. The trends in Osteichthyes after the PTBME contrast with the 'lilliput effect' proposed for some groups (e.g., Mutter and Neuman, 2009) and the long-term size increase of several fish clades in marine environments (Cope's rule; Guinot and Cavin, 2018).

A qualitative examination of the collected actinopterygians and actinistians from the Candelaria Hills shows that all belonged to mid-sized or large individuals, hence falling in line with the global pattern at the time. Among the undescribed fossils is a ~30 cm long skull of a coelacanth (PIMUZ A/I 4718), which pertained to one of the largest fishes of the Induan (cf., Scheyer et al., 2014, fig. 1c). The Griesbachian and Dienerian record of bony fishes is biased by taxa from Greenland and Madagascar, where large-sized forms (≥ 50 cm) are exceptional (Stensiö, 1932; Nielsen, 1942, 1949; Lehman, 1952; Beltan, 1980b; Kogan and Romano, 2016a). Very large bony fishes (≥ 1.5 m) were seemingly absent before the Smithian (Scheyer et al., 2014; Romano et al., 2017). Small osteichthyans were also not documented from other Early Triassic sites in the western United States, with the exception of Tanner (1936), whose material reportedly comes from the Woodside Formation, which is mainly continental (Hofmann et al., 2014). The absence of small, marine bony fishes in low latitudes is unusual and contrasts with the present latitudinal size distribution (Fisher et al., 2010).

Which factors led to the prevalence of large-bodied osteichthyans during the Early Triassic (pre-Spathian), a time of generally warm, but unstable global climate (e.g., Romano et al., 2013), and which factors to the radiation of small species (predominantly neopterygians and 'subholosteans;' Romano et al., 2016a; Smithwick and Stubbs, 2018) in the Middle Triassic requires further study. Being aquatic ectotherms, body size of fishes is determined primarily by temperature and bioavailability of oxygen, as well as food availability and quality (Verberk and Atkinson, 2013). The Early Triassic pattern is at odds with the mostly negative impact of current global warming on fish body size, although the present-day size reduction is co-influenced by selection pressure from sustained fishing by humans (e.g., Sheridan and Bickford, 2011). Modern-day exceptions (i.e., taxa increasing body size with warming) are found among organisms from higher latitudes and among secondary consumers (Sheridan and Bickford, 2011). Besides climatic constraints, ecological factors, such as the absence of marine tetrapod predators prior to the Spathian (Scheyer et al., 2014), could also account for the observed body size changes in Osteichthyes.

Conclusions

New fossil material can hold critical information regarding the timing of clade origins and evolutionary trajectories. This applies especially to the undersampled and understudied Permian–Triassic bony fish record (e.g., Sallan, 2014; Romano et al., 2016a). The presented, middle to late Dienerian actinopterygians from the new Candelaria Hills fossil bonanza comprise a new species of *Pteronisculus* White, 1933, a ptycholepid (*Ardoreosomus* n. gen.), and a parasemionotid neopterygian (*Candelarialepis* n. gen.), and probably more taxa are to be discovered in future studies. Curiously, more than half of the collected specimens are actinistians (coelacanths). *Pteronisculus nevadanus* n. sp. shows the apomorphic lachrymal contributing

https://doi.org/10.1017/jpa.2019.18 Published online by Cambridge University Press

to the oral margin, and is distinguished from other species by a unique set of characters. *Ardoreosomus* n. gen. exhibits typical ptycholepid features, but is distinct from other taxa, especially in its more oblique suspensorium (evidenced by the shape of the preopercle and hyomandibula) and lack of an elongate opercular process. *Candelarialepis* n. gen. resembles other parasemionotids, but stands out due to its large, bipartite preopercle and the peculiar ornamentation of the anterodorsal scales. The described taxa belong to groups that reached global distribution rapidly after the PTBME, thus confirming enhanced cosmopolitanism in Early Triassic (pre-Spathian) Osteichthyes.

Research on Early Triassic Osteichthyes from low-latitudinal localities is key to assess the atypical latitudinal diversity gradient, in which genus richness was greater in mid-latitudes than in low-latitudes. The Candelaria Hills material, together with other, recently published occurrences in Nevada (Elko County) and Idaho (Bear Lake County), provides evidence that the Early Triassic osteichthyan diversity in the subequatorial, eastern Panthalassa is still not well known. These data stress that sampling or preservational bias cannot be dismissed as contributing factors for the observed latitudinal diversity gradient. The Candelaria Hills material lacks small-bodied taxa. It thus mirrors the pattern documented at other marine, pre-Spathian localities, implying a biological signal (i.e., that other animals predominated in the small consumer guilds in shelf environments). We conclude that more research is necessary to understand the unusual spatiotemporal changes in osteichthyan diversity and body size after Earth's most severe mass extinction event of the past. The Candelaria Formation preserves invertebrates, bony fishes, and coprolites, the study of which can yield fresh insights into the poorly known Early Triassic ecosystems from low latitudes.

Acknowledgments

This contribution benefitted from constructive comments by L. Cavin, T. Bürgin, and the editors. We appreciate discussions with H. Bucher, T. Argyriou, M. Leu, T. Brühwiler (all PIMUZ), R. Hofmann (Museum für Naturkunde, Berlin, Germany), I. Kogan (TU Freiberg, Germany), and A. Brayard (Université de Bourgogne, Dijon, France). We thank S.G. Lucas (NMMNH) for the loan of specimens, and R. Roth (PIMUZ), L. Pauli, and J. Huber (both formerly PIMUZ) for lab work and help during preparation of fossils and casts. M. Véran and G. Clément (both MNHN.F) are thanked for assistance during collection visits. CR is grateful to I.R. Frick and C. and E. Romano-Turgut for their support. The Candelaria Hills collecting sites lie entirely on US public land (Bureau of Land Management). We thank BLM for allowing us to collect fossils under the auspices of Paleontological Resources Use Permit N-83484. We acknowledge support by the Swiss National Science Foundation (project numbers 120311/135075 and 144462 to WB and 200021/135446 to H. Bucher).

References

Agassiz, L., 1832, Untersuchungen über die fossilen Fische der Lias-Formation: Neues Jahrbuch für Mineralogie, Geognosie, Geologie und Petrefaktenkunde, v. 3, p. 139–149.

Agassiz, L., 1834, Abgerissene Bemerkungen über fossile Fische: Neues Jahrbuch für Mineralogie, Geognosie, Geologie und Petrefaktenkunde, v. 1834, p. 379–390.

Aldinger, H., 1937, Permische Ganoidfische aus Ostgrönland: Meddelelser om Grønland, v. 102, p. 1–392.

Anderson, K., and Woods, A.D., 2013, Taphonomy of Early Triassic fish fossils of the Vega-Phroso Siltstone Member of the Sulphur Mountain Formation near Wapiti Lake, British Columbia, Canada: Journal of Palaeogeography, v. 2, p. 321–343.

Arratia, G., 2009, Identifying patterns of diversity of the actinopterygian fulcra: Acta Zoologica, v. 90 (Supplement 1), p. 220–235.

Arratia, G., and Herzog, A., 2007, A new halecomorph fish from the Middle Triassic of Switzerland and its systematic implications: Journal of Vertebrate Paleontology, v. 27, p. 838–849.

Arratia, G., and Schultze, H.-P., 1991, Palatoquadrate and its ossifications: development and homology within osteichthyans: Journal of Morphology, v. 208, p. 1–81.

Baresel, B., Bucher, H., Bagherpour, B., Brosse, M., Guodun, K., and Schaltegger, U., 2017, Timing of global regression and microbial bloom linked with the Permian-Triassic boundary mass extinction: implications for driving mechanisms: Scientific Reports, v. 7, 43630.

Bassani, F., 1886, Sui fossili e sull'età degli schisti bituminosi Triasici di Besano in Lombardia. Communicazione preliminare: Atti della Società Italiana di Scienze Naturale, v. 29, p. 15–72.

Beltan, L., 1968, La faune ichthyologique de l'Eotrias du N.W. de Madagascar: le neurocrâne: Paris, Cahiers de Paléontologie CNRS, 135 p.

Beltan, L., 1980a, Sur la présence d'un poisson volant, *Icarealcyon malagasius*, n.g. n.sp. dans l'Eotrias malgache: Congrès Géologique International, v. 26, p. 155.

Beltan, L., 1980b, Eotrias du nord-ouest de Madagascar: etude de quelques poissons, dont un est en parturition: Annales de la Société Géologique du Nord, v. 99, p. 453–464.

Beltan, L., 1984a, Quelques poisons du Muschelkalk supérieur d'Espagne: Acta Geologica Hispánica, v. 19, p. 117–127.

Beltan, L., 1984b, A propos d'un poisson volant biplane de l'Eotrias du NW de Madagascar: Annales de la Société Géologique du Nord, v. 103, p. 75–82.

Bender, P., 2004, Late Permian actinopterygian (palaeoniscid) fishes from the Beaufort Group, South Africa: biostratigraphic and biogeographic implications: Council for Geoscience Bulletin, v. 135, p. 1–84.

Bittner, A., 1901, Über *Pseudomonotis Telleri* und verwandte Arten der unteren Trias: Jahrbuch der Kaiserlich-Königlichen Geologischen Reichsanstalt, v. 50, p. 559–592.

Blainville, H. de, 1818, Sur les ichthyolites ou les poissons fossils: Nouveau Dictionnaire d'Histoire Naturelle, appliquée aux Arts, à l'Agriculture, à l'Économie rurale et domestique, à la Medicine, etc. Nouvelle Edition, v. 27, p. 310–395.

Bock, W., 1959, New eastern American Triassic fishes and Triassic correlations: Geological Center Research Studies, v. 1, p. 1–184.

Boni, A., 1937, Vertebrati retici italiani: Memorie della Reale Accademia Nazionale dei Lincei, Serie 6, v. 6, p. 521–719.

Brayard, A., Bucher, H., Escarguel, G., Fluteau, F., Bourquin, S., and Galfetti, T., 2006, The Early Triassic ammonoid recovery: paleoclimatic significance of diversity gradients: Palaeogeography, Palaeoclimatology, Palaeoecology, v. 239, p. 374–395.

Brayard, A., Krumenacker, L.J., Botting, J.P., Jenks, J.F., Bylund, K.G., Fara, E., Vennin, E., Olivier, N., Goudemand, N., Saucède, T., Charbonnier, S., Romano, C., Doguzhaeva, L., Thuy, B., Hautmann, M., Stephen, D.A., Thomazo, C., and Escarguel, G., 2017, Unexpected Early Triassic marine ecosystem and the rise of the modern evolutionary fauna: Science Advances, v. 3, e1602159.

Brinkmann, W., Romano, C., Bucher, H., Ware, D., and Jenks, J., 2010, Palaeobiogeography and stratigraphy of advanced gnathostomian fishes (Chondrichthyes and Osteichthyes) in the Early Triassic and from selected Anisian localities (Report 1863–2009): Zentralblatt für Geologie und Paläontologie, Teil II, v. 2009, p. 765–812.

Brough, J., 1933, On a new palaeoniscid genus from Madagascar: Annals and Magazine of Natural History, Series 10, v. 11, p. 76–87.

Brough, J., 1936, On the evolution of bony fishes during the Triassic period: Biological Reviews, v. 11, p. 385–405.

Brough, J., 1939, The Triassic fishes of Besano, Lombardy: London, British Museum (Natural History), 117 p.

Bürgin, T., 1992, Basal ray-finned fishes (Osteichthyes; Actinopterygii) from the Middle Triassic of Monte San Giorgio (Canton Tessin, Switzerland). Systematic palaeontology with notes on functional morphology and palaeoecology: Schweizerische Paläontologische Abhandlungen, v. 114, p. 1–164.

Bürgin, T., 1999, Middle Triassic marine fish faunas from Switzerland, *in* Arratia, G., and Schultze, H.-P., eds., Mesozoic Fishes 2. Systematics and Fossil Record: München, Dr. Friedrich Pfeil, p. 481–494.

Ceballos, G., and Ehrlich, P.R., 2018, The misunderstood sixth mass extinction: Science, v. 360, p. 1080–1081.

https://doi.org/10.1017/jpa.2019.18 Published online by Cambridge University Press

Clarke, J.T. and Friedman, M., 2018, Body-shape diversity in Triassic–Early Cretaceous neopterygian fishes: sustained holostean disparity and predominantly gradual increases in teleost phenotypic variety: Paleobiology, v. 44, p. 402–433.
Cope, E.D., 1887, Geology and palaeontology. Zittel's Manual of Palaeontology: American Naturalist, v. 22, p. 1014–1019.
Collinson, J.W., and Hasenmueller, W.A., 1978, Early Triassic paleogeography and biostratigraphy of the Cordilleran miogeosyncline, *in* Howell, D.G., and McDougall, K.A., eds., Mesozoic Paleogeography of the Western United States. Pacific Coast Paleogeography Symposium 2: Los Angeles, The Pacific Section, Society of Economic Paleontologists and Mineralogists, p. 175–187.
Davies, G.R., Moslow, T.F., and Sherwin, M.D., 1997, Ganoid fish *Albertonia* sp. from the Lower Triassic Montney Formation, western Canada sedimentary basin: Bulletin of Canadian Petroleum Geology, v. 45, p. 715–718.
Deecke, W., 1889, Ueber Fische aus verschiedenen Horizonten der Trias: Palaeontographica, v. 35, p. 97–138.
Deecke, W., 1927, Über die Triasfische: Paläontologische Zeitschrift, v. 8, p. 184–198.
Fisher, J.A.D., Frank, K.T., and Leggett, W.C., 2010, Global variation in marine fish body size and its role in biodiversity-ecosystem functioning: Marine Ecology Progress Series, v. 405, p. 1–13.
Galfetti, T., Bucher, H., Ovtcharova, M., Schaltegger, U., Brayard, A., Brühwiler, T., Goudemand, N., Weissert, H., Hochuli, P.A., Cordey, F., and Guodun, K., 2007, Timing of the Early Triassic carbon cycle perturbations inferred from new U-Pb ages and ammonoid biochronozones: Earth and Planetary Science Letters, v. 258, p. 593–604.
Gardiner, B.G., 1966, Catalogue of Canadian fossil fishes: Contribution/Royal Ontario Museum, Toronto, Life Sciences Division, v. 68, p. 1–154.
Gardiner, B.G., 1967, Further notes on palaeoniscoid fishes with a classification of the Chondrostei: Bulletin of the British Museum (Natural History), v. 14, p. 143–206.
Gardiner, B.G., 1984, The relationships of the palaeoniscid fishes, a review based on new specimens of *Mimia* and *Moythomasia* from the Upper Devonian of Western Australia: Bulletin of the British Museum (Natural History), Geology Series, v. 37, p. 173–428.
Gardiner, B.G., and Jubb, R.A., 1975, A new palaeoniscid from the Lower Beaufort Series of South Africa: Annals of the South African Museum, v. 67, p. 441–445.
Gibson, S.Z., 2013, A new hump-backed ginglymodian fish (Neopterygii, Semionotiformes) from the Upper Triassic Chinle Formation of southeastern Utah: Journal of Vertebrate Paleontology, v. 33, p. 1037–1050.
Giles, S., Xu, G.-H., Near, T.J., and Friedman, M., 2017, Early members of 'living fossil' lineage imply later origin of modern ray-finned fishes: Nature, v. 549, p. 265–268.
Goddard, M., 1907, Fish remains from the marine Lower Triassic of Aspen Ridge, Idaho: University of California Publications, Bulletin of the Department of Geology, v. 5, p. 145–148.
Grande, L., 2010, An empirical synthetic pattern study of gars (Lepisosteiformes) and closely related species, based mostly on skeletal anatomy: the resurrection of Holostei: American Society of Ichthyology and Herpetology, Special Publication, v. 6, p. 1–871.
Grande, L., and Bemis, W.E., 1998, A comprehensive phylogenetic study of amiid fishes (Amiidae) based on comparative skeletal anatomy. An empirical search for interconnected patterns of natural history: Society of Vertebrate Paleontology Memoir, v. 4, p. 1–690.
Griffith, J., 1977, Upper Triassic fishes from Polzberg bei Lunz, Austria: Zoological Journal of the Linnean Society, v. 60, p. 1–93.
Guinot, G., and Cavin, L., 2018, Body size evolution and habitat colonization across 100 million years (Late Jurassic–Paleocene) of the actinopterygian evolutionary history: Fish and Fisheries, v. 19, p. 577–597.
Hautmann, M., 2014, Diversification and diversity partitioning: Paleobiology, v. 40, p. 162–176.
Hilton, E.J., Grande, L., and Bemis, W.E., 2011, Skeletal anatomy of the shortnose sturgeon, *Acipenser brevirostrum* Lesueur, 1818, and the systematics of sturgeons (Acipenseriformes, Acipenseridae): Fieldiana: Life and Earth Sciences, v. 3, p. 1–168.
Hofmann, R., Hautmann, M., Brayard, A., Nützel, A., Bylund, K.G., Jenks, J.F., Vennin, E., Olivier, N., and Bucher, H., 2014, Recovery of benthic marine communities from the end-Permian mass extinction at the low latitudes of eastern Panthalassa: Palaeontology, v. 57, p. 547–589.
Huxley, T.H., 1880, On the application of the laws of evolution to the arrangement of the vertebrata, and more particularly of the Mammalia: Proceedings of the Scientific Meetings of the Zoological Society of London, v. 1880, p. 649–662.
Knopf, A., 1922, The Candelaria silver district, Nevada: U.S. Geological Survey Bulletin, v. 735a, p. 1–22.
Kogan, I., and Romano, C., 2016a, Redescription of *Saurichthys madagascariensis* Piveteau, 1945 (Actinopterygii, Early Triassic), with implications for the early saurichthyid morphotype: Journal of Vertebrate Paleontology, v. 36, e1151886.
Kogan, I., and Romano, C., 2016b, A new postcranium of *Saurichthys* from the Early Triassic of Spitsbergen. Paläontologie, Stratigraphie, Fazies, 23: Freiberger Forschungshefte C, v. 550, p. 205–221.
Koot, M.B., 2013, Effects of the Late Permian mass extinction on chondrichthyan palaeobiodiversity and distribution patterns [Ph.D. thesis]: Plymouth, Plymouth University, 853 p. http://pearl.plymouth.ac.uk/handle/10026.1/1584
Lambe, L.M., 1916, Ganoid fishes from near Banff, Alberta: Proceedings and Transactions of the Royal Society of Canada, Series III, v. 10, p. 35–44.
Lehman, J.-P., 1952, Etude complémentaire des poissons de l'Eotrias de Madagascar: Kungliga Svenska Vetenskapsakademiens Handlingar, Fjärde Serien, v. 2(6), p. 1–201.
Lehman, J.-P., Château, C., Laurain, M., and Nauche, M., 1959, Paléontologie de Madagascar 27. Les poissons de la Sakamena moyenne: Annales de Paléontologie, v. 45, p. 175–219.
Leidy, J., 1857, Notices of some remains of extinct fishes: Proceedings of the Academy of Natural Sciences of Philadelphia, v. 9, p. 167–168.
Li, Q., 2009, A new parasemionotid-like fish from the Lower Triassic of Jurong, Jiangsu Province, South China: Palaeontology, v. 52, p. 369–384.
Linnaeus, C., 1758, Systema Naturae, Editio X [Systema naturae per regna tria naturae, secundum classes, ordines, genera, species, cum characteribus, differentiis, synonymis, locis. Tomus 1. Editio decima, reformata]. Laurentii Salvii: Holmiæ (1956 facsimile reprint; London, Trustees of the British Museum [Natural History]).
Linnaeus, C., 1766, Systema Naturae. Editio Duodecima, Reformata. Impensis Direct Laurentii Salvi: Holmiae, v. 1, p. 1–532.
Liu, G.-B., Feng, H.-Z., Wang, J.-X., Wu, T.-M., and Zhai, Z.-H., 2002, Early Triassic fishes from Jurong, Jiangsu: Acta Palaeontologica Sinica, v. 41, p. 27–52 [in Chinese, with English summary].
Liu, H., and Ma, T., 1973, A new palaeoniscoid fish from the Chichitsao series (Permian) of Sinkiang: Memoirs of the Institute of Vertebrate Paleontology and Paleoanthropology, Academia Sinica, v. 10, p. 6–14 [in Chinese].
López-Arbarello, A., 2004, The record of Mesozoic fishes from Gondwana (excluding India and Madagascar), *in* Arratia, G., and Tintori, A., eds., Mesozoic fishes 3. Systematics, Paleoenvironments and Biodiversity: München, Dr. Friedrich Pfeil, p. 597–624.
López-Arbarello, A., Bürgin, T., Furrer, H., and Stockar, R., 2016, New holostean fishes (Actinopterygii: Neopterygii) from the Middle Triassic of the Monte San Giorgio (Canton Ticino, Switzerland): PeerJ, v. 4, e2234.
Marramà, G., Lombardo, C., Tintori, A., and Carnevale, G., 2017, Redescription of '*Perleidus*' (Osteichthyes, Actinopterygii) from the Early Triassic of northwestern Madagascar: Rivista Italiana di Paleontologia e Stratigrafia, v. 123, p. 219–242.
Mickle, K.E., 2013, Revisiting the actinopterygian preopercle, *in* Arratia, G., Schultze, H.-P., and Wilson, M.V.H., eds., Mesozoic Fishes 5. Global Diversity and Evolution: München, Dr. Friedrich Pfeil, p. 35–71.
Mickle, K.E., 2015, Identification of the bones of the snout in fossil lower actinopterygians—a new nomenclature scheme based on characters: Copeia, v. 103, p. 838–857.
Müller, J., 1845, Ueber den Bau und die Grenzen der Ganoiden, und über das natürliche System der Fische: Archiv für Naturgeschichte, v. 11, p. 91–141.
Müller, A.H., 1962, Körperlich erhaltene Fische (Palaeoniscoidea) aus dem Zechstein (Kupferschiefer) von Ilmenau (Thüringen): Geologie, v. 11, p. 845–856.
Muller, S.W., and Ferguson, H.G., 1939, Mesozoic stratigraphy of the Hawthorne and Tonopah quadrangles, Nevada: Bulletin of the Geological Society of America, v. 50, p. 1573–1624.
Mutter, R., 2011, A case study of the palaeobiogeography of Early Mesozoic actinopterygians, the family Ptycholepidae, *in* Upchurch, P., McGowan, A.J., and Slater, C.S.C., eds., Palaeogeography and Palaeobiogeography: Biodiversity in Space and Time: Boca Raton, CRC Press, p. 143–171.
Mutter, R., and Neuman, A.G., 2009, Recovery from the end-Permian extinction event: evidence from "Lilliput *Listracanthus*": Palaeogeography, Palaeoclimatology, Palaeoecology, v. 284, p. 22–28.
Mutter, R., Cartanyà, J., and Basaraba, S.A.U., 2008, New evidence of *Saurichthys* from the Lower Triassic with an evaluation of early saurichthyid diversity, *in* Arratia, G., Schultze, H.-P., and Wilson, M.V.H., eds., Mesozoic Fishes 4. Homology and Phylogeny: München, Dr. Friedrich Pfeil, p. 103–127.
Neuman, A.G., 2015, Fishes from the Lower Triassic portion of the Sulphur Mountain Formation in Alberta, Canada: geological context and taxonomic composition: Canadian Journal of Earth Sciences, v. 52, p. 557–568.
Neuman, A.G., and Mutter, R.J., 2005, *Helmolepis cyphognathus*, sp. nov., a new platysiagid actinopterygian from the Lower Triassic Sulphur Mountain Formation (British Columbia, Canada): Canadian Journal of Earth Sciences, v. 42, p. 25–36.

Newberry, J.S., 1878, Descriptions of new fossil fishes from the Trias: Annals of the New York Academy of Sciences, v. 1, p. 127–128.
Nielsen, E., 1936, Some few preliminary remarks on Triassic fishes from East Greenland: Meddelelser om Grønland, v. 112, no. 3, p. 1–55.
Nielsen, E., 1942, Studies on Triassic Fishes from East Greenland 1. *Glaucolepis* and *Boreosomus*: Palaeozoologica Groenlandica, v. 1, p. 1–403.
Nielsen, E., 1949, Studies on Triassic fishes from East Greenland 2. *Australosomus* and *Birgeria*: Palaeozoologica Groenlandica, v. 3, p. 1–309.
Nielsen, E., 1961, On the Eotriassic fish faunas of central east Greenland, *in* Raasch, G.O., ed., Geology of the Arctic 1. Proceedings of the First International Symposium on Arctic Geology: Toronto, University Press, p. 255–257.
Nybelin, O., 1977, Studies on Triassic fishes from East Greenland III—on *Helmolepis gracilis* Stensiö: Meddelelser om Grønland, v. 200, no. 2, p. 1–14.
Olsen, P.E., 1984, The skull and pectoral girdle of the parasemionotid fish *Watsonulus eugnathoides* from the Early Triassic Sakamena Group of Madagascar, with comments on the relationships of holostean fishes: Journal of Vertebrate Paleontology, v. 4, p. 481–499.
Orchard, M.J., and Zonneveld, J.-P., 2009, The Lower Triassic Sulphur Mountain Formation in the Wapiti Lake area: lithostratigraphy, conodont biostratigraphy, and a new biozonation for the lower Olenekian (Smithian): Canadian Journal of Earth Sciences, v. 46, p. 757–790.
Ørvig, T., 1978, Microstructure and growth of the dermal skeleton in fossil actinopterygian fishes: *Boreosomus*, *Plegmolepis* and *Gyrolepis*: Zoologica Scripta, v. 7, p. 125–144.
Ovtcharova, M., Bucher, H., Schaltegger, U., Galfetti, T., Brayard, A., and Guex, J., 2006, New Early to Middle Triassic U-Pb ages from South China: calibration with ammonoid biochronozones and implications for the timing of the Triassic biotic recovery: Earth and Planetary Science Letters, v. 243, p. 463–475.
Page, B.M., 1959, Geology of the Candelaria mining district, Mineral County, Nevada: Nevada Bureau of Mines, Bulletin, v. 56, p. 1–67.
Patterson, C., 1982, Morphology and interrelationships of primitive actinopterygian fishes: American Zoologist, v. 22, p. 241–259.
Payne, J.L., Bush, A.M., Heim, N.A., Knope, M.L., and McCauley, D.J., 2016, Ecological selectivity of the emerging mass extinction in the oceans: Science, v. 353, p. 1284–1286.
Payne, J.L., and Clapham, M.E., 2012, End-Permian mass extinction in the oceans: an ancient analog for the twenty-first century?: Annual Reviews in Earth and Planetary Science, v. 40, p. 89–111.
Piveteau, J., 1934, Paléontologie de Madagascar 21. Les poissons du Trias inférieur. Contribution à l'études des actinopterygians: Annales de Paléontologie, v. 23, p. 83–178.
Piveteau, J., 1935, Ressemblances des faunes ichthyologiques du Groenland et du Spitzberg avec celle de Madagascar, au Trias inférieur: Compte Rendu Sommaire des Séances de la Société Géologique de France, v. 1935, p. 113–114.
Poole, F.G., and Wardlaw, B.R., 1978, Candelaria (Triassic) and Diablo (Permian) formations in southern Toquima Range, Central Nevada, *in* Howell, D.G., and McDougall, K.A., eds., Mesozoic Paleogeography of the Western United States. Pacific Coast Paleogeography Symposium 2: Los Angeles, The Pacific Section, Society of Economic Paleontologists and Mineralogists, p. 271–276.
Priem, F., 1924, Paléontologie de Madagascar 12. Les poisons fossils: Annales de Paléontologie, v. 13, p. 107–132.
Puttick, M.N., Kriwet, J., Wen, W., Hu, S., Thomas, G.H., and Benton, M.J., 2017, Body length of bony fishes was not a selective factor during the biggest mass extinction of all time: Palaeontology, v. 60, p. 727–741.
Regan, C.T., 1923, The skeleton of *Lepidosteus*, with remarks on the origin and evolution of the lower neopterygian fishes: Proceedings of the Zoological Society of London, v. 93, p. 445–461.
Romano, C., Kogan, I., Jenks, J., Jerjen, I., and Brinkmann, W., 2012, *Saurichthys* and other fossil fishes from the late Smithian (Early Triassic) of Bear Lake County (Idaho, USA), with a discussion of saurichthyid palaeogeography and evolution: Bulletin of Geosciences, v. 87, p. 543–570.
Romano, C., Goudemand, N., Vennemann, T.W., Ware, D., Schneebeli-Hermann, E., Hochuli, P.A., Brühwiler, T., Brinkmann, W., and Bucher, H., 2013, Climatic and biotic upheavals following the end-Permian mass extinction: Nature Geoscience, v. 6, p. 57–60.
Romano, C., Koot, M.B., Kogan, I., Brayard, A., Minikh, A.V., Brinkmann, W., Bucher, H., and Kriwet, J., 2016a, Permian–Triassic Osteichthyes (bony fishes): diversity dynamics and body size evolution: Biological Reviews, v. 91, p. 106–147.
Romano, C., Ware, D., Brühwiler, T., Bucher, H., and Brinkmann, W., 2016b, Marine Early Triassic Osteichthyes from Spiti, Indian Himalayas: Swiss Journal of Palaeontology, v. 135, p. 275–294.
Romano, C., Jenks., J.F., Jattiot, R., Scheyer, T.M., Bylund, K.G., and Bucher, H., 2017, Marine Early Triassic Actinopterygii from Elko County (Nevada, USA): implications for the Smithian equatorial vertebrate eclipse: Journal of Paleontology, v. 91, p. 1025–1046.
Romano, C., Argyriou, T., Krumenacker, L.J., and the Paris Biota Team, in press, Chondrichthyan teeth from the Early Triassic Paris Biota (Bear Lake County, Idaho, USA): Geobios, doi:https://doi.org/10.1016/j.geobios.2019.04.001.
Rosen, D.E., Forey, P.L., Gardiner, B.G., and Patterson, C., 1981, Lungfishes, tetrapods, paleontology, and plesiomorphy: Bulletin of the American Museum of Natural History, v. 169, p. 159–276.
Sallan, L.C., 2014, Major issues in the origins of ray-finned fish (Actinopterygii) biodiversity: Biological Reviews, v. 89, p. 950–971.
Schaeffer, B., 1952, The palaeoniscoid fish *Turseodus* from the Upper Triassic Newark Group: American Museum Novitates, v. 1581, p. 1–24.
Schaeffer, B., 1967, Late Triassic fishes from the western United States: Bulletin of the American Museum of Natural History, v. 35, p. 285–342.
Schaeffer, B., and Mangus, M., 1976, An Early Triassic fish assemblage from British Columbia: Bulletin of the American Museum of Natural History, v. 156, p. 127–216.
Schaeffer, B., Dunkle, D.H., and McDonald, N.G., 1975, *Ptycholepis marshi* Newberry, a chondrostean fish from the Newark Group of eastern North America: Fieldiana, Geology, v. 33, p. 205–233.
Scheyer, T.M., Romano, C., Jenks, J., and Bucher, H., 2014, Early Triassic marine biotic recovery: the predators' perspective: PLoS ONE, v. 9, e88987.
Schultze, H.-P., 2008, Nomenclature and homologization of cranial bones in actinopterygians, *in* Arratia, G., Schultze, H.-P., and Wilson, M.V.H., eds., Mesozoic Fishes 4. Homology and Phylogeny: München, Dr. Friedrich Pfeil, p. 23–48.
Sheridan, J.A., and Bickford, D., 2011, Shrinking body size as an ecological response to climate change: Nature Climate Change, v. 1, p. 401–406.
Smithwick, F.M., and Stubbs, T.L., 2018, Phanerozoic survivors: actinopterygian evolution through the Permo-Triassic and Triassic-Jurassic mass extinction events: Evolution, v. 72, p. 348–362.
Stensiö, E., 1921, Triassic fishes from Spitzbergen 1: Wien, Adolf Holzhausen, 307 p.
St. Hilaire, E.G., 1802. Histoire naturelle et description anatomique d'un nouveau genre de poisson du Nil nommé Polyptère: Musée Histoire Naturelle, Paris, v. 1, p. 57–68.
Stensiö, E., 1932. Triassic fishes from East Greenland 1–2: Meddelelser om Grønland, v. 83, no. 3, p. 1–305.
Su, T.-T., 1974, New Jurassic ptycholepid fishes from Szechuan, S.W. China: Vertebrata PalAsiatica, v. 12, p. 1–20.
Su, T.-T., 1993, New Jurassic ganoid fishes from northwestern Gansu, China: Vertebrata PalAsiatica, v. 31, p. 1–14.
Sun, Z., Tintori, A., Yaozhong, X., Lombardo, C., Peigang, N., and Dayong, J., 2017, A new non-parasemionotiform order of the Halecomorphi (Neopterygii, Actinopterygii) from the Middle Triassic of Tethys: Journal of Systematic Palaeontology, v. 15, p. 223–240.
Tanner, V.M., 1936, A study of Utah fossil fishes with the description of a new genus and species: Proceedings of the Utah Academy of Sciences, Arts and Letters, v. 13, p. 81–89.
Tintori, A., 1990, The actinopterygian fish *Prohalecites* from the Triassic of northern Italy: Palaeonotology, v. 33, p. 155–174.
Tintori, A., Hitij, T., Jiang, D.-Y., Lombardo, C., and Sun, Z.-Y., 2014, Triassic actinopterygian fishes: the recovery after the end-Permian crisis: Integrative Zoology, v. 9, p. 394–411.
Tintori, A., Lombardo, C., and Kustatscher, E., 2016, The Pelsonian (Anisian, Middle Triassic) fish assemblage from Monte Prà della Vacca/Kühwiesenkopf (Braies Dolomites, Italy): Neues Jahrbuch für Geologie und Paläontologie, Abhandlungen, v. 282, p. 181–200.
Tong, J., Zhou, X., Erwin, D.H., Zuo, J., and Zhao, L., 2006, Fossil fishes from the Lower Triassic of Majiashan, Chaohu, Anhui Province, China: Journal of Paleontology, v. 80, p. 146–161.
Tozer, E.T., 1965, Lower Triassic stages and ammonoid zones of Arctic Canada: Paper of the Geological Survey of Canada, v. 65, p. 1–14.
Uyeno, T., 1978, On some Lower Triassic fishes from Ankilokara, Madagascar: Bulletin of the National Science Museum, Series C (Geology & Paleontology), v. 4, p. 193–198.
Véran, M., 1988, Les éléments accessoires de l'arc hyoïdien des poissons téléostomes (Acanthodiens et Osteichthyens) fossiles et actuels: Mémoires du Muséum Nationale d'Histoire Naturelle, Série C, v. 54, p. 1–88.
Véran, M., 1996, Le labial des poissons actinoptérygiens fossiles et actuels: Bulletin du Muséum Nationale d'Histoire Naturelle, 4ième Série, Séction C, v. 18, p. 1–55.
Verberk, W.C.E.P., and Atkinson, D., 2013, Why polar gigantism and Palaeozoic gigantism are not equivalent: effects of oxygen and temperature on the body size of ectotherms: Functional Ecology, v. 27, p. 1275–1285.
Vogt, C., 1851, Zoologische Briefe. Naturgeschichte der lebenden und untergegangenen Thiere, für Lehrer, höhere Schulen und Gebildete aller Stände II: Frankfurt am Main, Literarische Anstalt, 640 p.
von Krafft, A., and Diener, C., 1909, Lower Triassic Cephalopoda from Spiti, Malla, Johar, and Byans: Palaeontologia Indica v. 6, p. 1–186.

https://doi.org/10.1017/jpa.2019.18 Published online by Cambridge University Press

Wade, R.T., 1935, The Triassic fishes of Brookvale, New South Wales: London, British Museum (Natural History), 92 p.
Wade, R.T., 1940, Australian Triassic fishes: Journal and Proceedings of the Royal Society of New South Wales, v. 74, p. 377–396.
Ware, D., Jenks, J.F., Hautmann, M., and Bucher, H., 2011, Dienerian (Early Triassic) ammonoids from the Candelaria Hills (Nevada, USA) and their significance for palaeobiogeography and palaeoceanography: Swiss Journal of Geosciences, v. 104, p. 161–181.
Ware, D., Bucher, H., Brayard, A., Schneebeli-Hermann, E., and Brühwiler, T., 2015, High-resolution biochronology and diversity dynamics of the Early Triassic ammonoid recovery: the Dienerian faunas of the Northern Indian Margin: Palaeogeography, Palaeoclimatology, Palaeoecology, v. 440, p. 363–373.
Ware, D., Bucher, H., Brühwiler, T., Schneebeli-Hermann, E., Hochuli, P.A., Roohi, G., Ur-Rehman, K., and Yaseen, A., 2018a, Griesbachian and Dienerian (Early Triassic) ammonoids from the Salt Range, Pakistan: Fossils and Strata, v. 63, p. 11–175.
Ware, D., Bucher, H., Brühwiler, T., and Krystyn, L., 2018b, Dienerian (Early Triassic) ammonoids from Spiti (Himachal Pradesh, India): Fossils and Strata, v. 63, p. 177–241.
Wen, W., Hu, S.X., Zhang, Q.Y., Benton, M.J., Kriwet, J., Chen, Z.Q., Zhou, C.Y., Xie, T., and Huang, J.Y., 2019, A new species of *Platysiagum* from the Luoping Biota (Anisian, Middle Triassic, Yunnan, South China) reveals the relationship between Platysiagidae and Neopterygii: Geological Magazine, v. 156, p. 669–682.
White, E.I., 1932, On a new Triassic fish from north-east Madagascar: Annals and Magazine of Natural History, Series 10, v. 10, p. 80–83.
White, E.I., 1933, New Triassic palaeoniscids from Madagascar: Annals and Magazine of Natural History, Series 10, v. 11, p. 118–128.
White, E.I., and Moy-Thomas, J.A., 1940, VII.—Notes on the nomenclature of fossil fishes. Part II. Homonyms D–L: Journal of Natural History, Series 11, v. 6, no. 31, p. 98–103.
Wignall, P.B., and Newton, R., 2003, Contrasting deep-water records from the Upper Permian and Lower Triassic of South Tibet and British Columbia: evidence for a diachronous mass extinction: Palaios, v. 18, p. 153–167.
Wyld, S.J., 2000, Triassic evolution of the arc and backarc of northwestern Nevada, and evidence for extensional tectonism, *in* Soreghan, M.J., and Gehrels, G.E., eds., Paleozoic and Triassic Paleogeography and Tectonics of Western Nevada and Northern California: Geological Society of America Special Paper, v. 347, p. 185–207.
Xu, G.-H., and Shen, C.-C., 2015, *Panxianichthys imparilis* gen. et sp. nov., a new ionoscopiform (Halecomorphi) from the Middle Triassic of Guizhou, China: Vertebrata PalAsiatica, v. 53, p. 1–15.
Xu, G.-H., Shen, C.-C., and Zhao, L.J., 2014, *Pteronisculus nielseni* sp. nov., a new stem-actinopteran fish from the Middle Triassic of Luoping, Yunnan Province, China: Vertebrata PalAsiatica, v. 52, p. 364–380.
Xu, G.-H., Gao, K.-Q., and Coates, M.I., 2015, Taxonomic revision of *Plesiofuro mingshuica* from the Lower Triassic of northern Gansu, China, and the relationships of early neopterygian clades: Journal of Vertebrate Paleontology, v. 35, e1001515.

Accepted: 2 March 2019